hyperresponsiveness and eosinophil infiltration, which are hallmarks of bronchial asthma. To determine the exact roles of α-CGRP in vivo, we chose to study the airway responsiveness and eosinophilia in α-CGRP gene-disrupted mice, which have been recently established (38). After sensitization and antigen challenge, we assessed airway responsiveness and measured proinflammatory mediators.

METHODS

Mice. α-CGRP-null mice were established as previously reported (38). Briefly, the mouse *CT/α-CGRP* genomic DNA was cloned from a BALB/c mouse genomic library in EMBL3 using synthetic oligonucleotide probes derived from the mouse *CT/α-CGRP* cDNA sequence. A 7.0-kb fragment containing exons 3–5 of the mouse *CT/α-CGRP* gene was subcloned into pBluescript (Stratagene). A targeting vector was constructed by replacing the 1.6-kb *Xba*I-*Xba*I fragment encompassing exon 5, which is specific for *α-CGRP*, with the neomycin resistance gene, and flanking the thymidine kinase gene. This plasmid was linearized with *Not*I and introduced into 129/Sv-derived SM-1 ES cells by electroporation; then the cells were selected in medium containing G418 and ganciclovir. Homologous recombinants were identified by PCR and Southern blot analysis. Targeted ES cell clones were injected into C57BL/6 mouse blastocysts to generate chimeric mice. Male chimeras were then cross bred with C57BL/6 females, and germline transmission was achieved. Mice heterozygous for α-CGRP-mutant allele with the genetic background of the 129/Sv × C57BL/6 hybrid were mated. Offspring were genotyped at 4 wk of age. For genotyping, genomic DNAs were isolated from biopsied tail and subjected to PCR amplification. The animals were maintained on a 7:20-h light-dark cycle at 23°C. Mice were fed a standard laboratory diet and water ad libitum. Mutant mice (α-$CGRP^{-/-}$) and their littermate controls (α-$CGRP^{+/+}$) were used in the present study.

Sensitization and antigen challenge. Mice were sensitized with an intraperitoneal injection of 0.5 ml of a solution containing 0.1 mg of ovalbumin (OA) complexed with aluminum hydroxide (2 mg/ml). On *day 8*, the mice were boosted with the same mixture. On *day 12*, these sensitized mice were challenged for 30 min with 1% OA in saline aerosol generated with an ultrasonic nebulizer (Ultra-Neb100, DeVilbiss, Somerset, PA). Control mice received an intraperitoneal injection of saline and saline aerosols in the same manner. Three days after the aerosol challenge, we measured bronchial responsiveness or performed bronchoalveolar lavage (BAL).

Animal preparation. Animals were anesthetized with pentobarbital sodium (25 mg/kg ip) and ketamine hydrochloride (25 mg/kg ip) in combination and then paralyzed with pancuronium bromide (0.3 mg/kg ip). Anesthesia and paralysis were maintained by supplemental administration of 10% of the initial dose every hour. After tracheostomy, a metal endotracheal tube (1 mm ID, 8 mm long) was inserted in the trachea. Animals were mechanically ventilated (model 683, Harvard Apparatus, South Natick, MA) with tidal volumes of 10 ml/kg and frequencies of 2.5 Hz. The thorax was widely opened by means of a midline sternotomy, and a positive end-expiratory pressure of 2 cmH_2O was applied by placing the expired line under water. During the experiments, O_2 gas was continuously supplied to the ventilatory system. Under these ventilatory conditions, arterial pH, P_{O_2}, and P_{CO_2} were 7.35–7.45, 100–180 mmHg, and 30–45 mmHg, respectively, at the end of experiments (Compact 3 blood gas analyzer, AVL Medical Systems). A heating pad was used to maintain the body temperature of animals.

Tracheal pressure was measured with a piezoresistive microtransducer (model 8510B-2, Endevco, San Juan Capistrano, CA) placed in the lateral port of the tracheal cannula. Tracheal flow was measured by means of a Fleisch pneumotachograph (Metabo, Lausanne, Switzerland). All signals were amplified, filtered at a cutoff frequency of 100 Hz, and converted from analog to digital with a converter (model DT2801-A, Data Translation, Marlborough, MA). The signals were sampled at a rate of 200 Hz and stored on an IBM-AT-compatible computer. Lung resistance (R_L) and elastance (E_L) were measured as previously described (27, 31, 32).

Airway responsiveness to methacholine administration. At the start of the protocol, two deep inhalations (3 times tidal volume) were delivered to standardize volume history. All animals were then challenged with saline aerosol for 2 min. Aerosols were generated by an ultrasonic nebulizer and delivered through the inspiratory line into the trachea. Measurements of 10-s duration were sampled during tidal ventilation 1 min after administration of saline aerosol. This represented the baseline measurement. Then each dose of methacholine (MCh) aerosol was administered for 2 min in a dose-response manner (0.625–20 mg/ml). Airway responsiveness was assessed using the concentration of MCh required to increase R_L to 200% of baseline values (30).

BAL fluid. BAL was performed [5 times with 1 ml of phosphate-buffered saline (PBS)] in each group. In each animal, 90% (4.5 ml) of the total injected volume was consistently recovered. After BAL fluid (BALF) was centrifuged at 450 *g* for 10 min, the total and differential cell counts of the BALF were determined from the cell fraction (29, 34, 35). The supernatant was stored at −70°C until assays were performed. The concentration of protein was measured by Lowry's method, with bovine serum albumin as a standard.

Assay of IgE in BALF. IgE levels in the BALF were determined using ELISA kits (Amersham Pharmacia Biotech, Piscataway, NJ). The detection limit of the ELISA assays for IgE was 10 ng/ml.

Assay of thromboxane and leukotriene in BALF. Thromboxane (Tx) A_2 (TxA_2, measured as TxB_2) and leukotriene (LT) $C_4/D_4/E_4$ were determined using enzyme immunoassay (EIA) kits (Amersham Pharmacia Biotech). The detection limits of the EIA assays for TxB_2 and $LTC_4/D_4/E_4$ were 3.6 and 10 pg/ml, respectively.

Assay of endothelin-1 in BALF. Endothelin-1 (ET-1) levels in the BALF were determined using EIA kits (IBL, Fujioka, Japan). The detection limit of the EIA assays for ET-1 was 0.78 pg/ml.

Assessment of CGRP immunoreactivity. In each group, the lungs of the mouse were removed intact and fixed with 10% formalin. After fixation, the tissue blocks obtained from midsagittal slices of the lungs were embedded in paraffin. Blocks were cut 4 μm thick by using a microtome. The preparations were processed for immunostaining by means of the avidin-biotin-peroxidase complex method. The slides were deparaffinized in a xylene bath and dehydrated in ethanol. Endogenous peroxidase activities were blocked by treatment with 0.6% H_2O_2 in 100% methanol for 30 min at room temperature. The primary antibody, rabbit anti-CGRP (rat) IgG (Peninsula Laboratories, San Carlos, CA), was diluted 1:200 in 10% FCS-PBS and added to the preparations overnight in a cold room. After six washes with PBS, the preparations were exposed to biotin-bound goat antiserum against rabbit IgG as the second antibody for 60 min at room temperature (Histofine, Nichirei, Tokyo, Japan). After the slides were washed with PBS, the tissues were incubated in horseradish peroxi-

dase-bound streptavidin for 45 min (Histofine). The peroxidase reaction was performed with 3,3′-diaminobenzidine tetrahydrochloride as a chromogen (Vector Laboratories, Burlingame, CA).

Sections were screened and graded using the immunoreactivity score by two observers who were blind to the status of the specimen (5, 21). Visual assessments of the density of CGRP immunoreactivity were graded from none (score = 0) to abundant (score = 4). To examine the location of CGRP immunoreactivity, we analyzed large airways (airway diameter >0.2 mm), small airways (airway diameter <0.1 mm), and lung parenchyma. The scores represent the density of CGRP-immunoreactive cells and tissues that might include nerves, ganglia, and neuroepithelial bodies (NEBs) (5). In terms of the reproducibility of this assessment, inter- or intraobserver variances were not significant.

Materials and chemicals. Materials and chemicals were obtained from Sigma Chemical (St. Louis, MO) unless otherwise specified.

Data analysis. Comparisons of data among the experimental groups were carried out with ANOVA (Scheffé's test). Values are means ± SE. $P < 0.05$ was taken as significant.

RESULTS

Airway responsiveness to MCh administration. There were no significant differences in baseline RL and EL among each group. MCh dose-response curves for RL and EL are demonstrated in Figs. 1 and 2, respectively.

Airway responsiveness was assessed using the MCh concentration required to increase RL to 200% of baseline: 17.4 ± 1.8 and 17.6 ± 1.4 mg/ml for saline-treated α-$CGRP^{+/+}$ and α-$CGRP^{-/-}$, respectively, and 6.9 ± 1.3 and 16.5 ± 1.5 mg/ml for OA-treated α-$CGRP^{+/+}$ and α-$CGRP^{-/-}$, respectively ($P < 0.05$, OA-treated α-$CGRP^{+/+}$ vs. other groups). Although bronchial hyperresponsiveness to MCh was observed in the OA-challenged wild-type mice, responses in the OA-challenged α-$CGRP^{-/-}$ mice were significantly reduced compared with the OA-challenged wild-type group.

Assessment of the BALF. Antigen exposure increased protein amount in BALF, although there was no difference between the wild-type and mutant mice (Fig. 3). Total cell counts and cell fractions in BALF are shown in Table 1, indicating the increases in the total cell number in the OA-sensitized groups. OA challenge induced eosinophil infiltration, whereas no differences in the fraction and number of BALF eosinophils were observed between the wild-type and α-$CGRP^{-/-}$ mice.

The IgE levels were significantly greater in OA- than in saline-treated mice. However, there were no significant differences between the wild-type and α-$CGRP^{-/-}$ mice (Fig. 4).

Measurements of thromboxane, leukotriene, and ET-1 in BALF. There were no significant differences in BALF TxB_2 among the groups: 0.140 ± 0.047 and 0.135 ± 0.076 ng in saline-treated α-$CGRP^{+/+}$ and α-$CGRP^{-/-}$, respectively, and 0.423 ± 0.204 and 0.498 ± 0.262 ng in OA-treated α-$CGRP^{+/+}$ and α-$CGRP^{-/-}$, respectively.

BALF $LTC_4/D_4/E_4$ was significantly greater in OA-treated $CGRP^{+/+}$ mice than in any other group (Fig. 5).

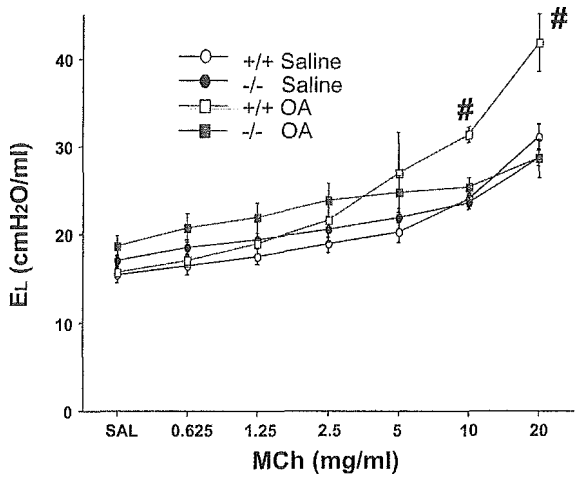

Fig. 2. MCh dose-response curves for lung elastance (EL) in wild-type and α-CGRP-deficient mice (n = 7–9). #$P < 0.05$ compared with other groups.

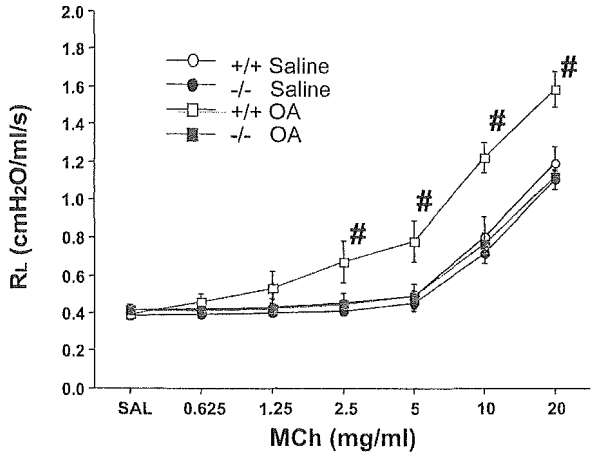

Fig. 1. Methacholine (MCh) dose-response curves for lung resistance (RL) in wild-type (+/+) mice and mice deficient in the α-isoform (−/−) of calcitonin gene-related peptide (α-CGRP) (n = 7–9). #$P < 0.05$ compared with other groups. OA, ovalbumin.

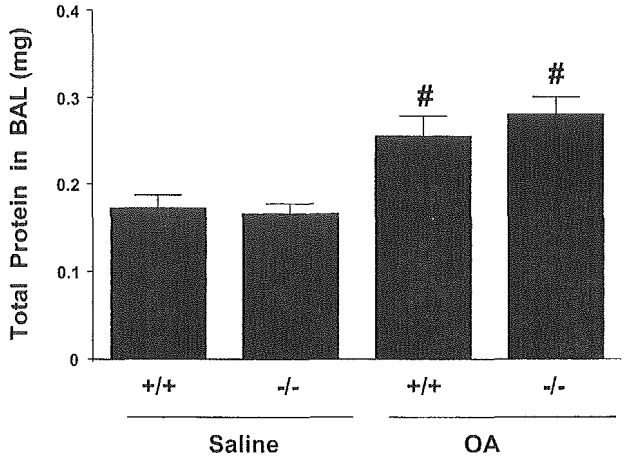

Fig. 3. Roles of CGRP in antigen-induced protein leakage. Protein leakage is assessed by total protein amount in bronchoalveolar lavage (BAL) fluid in wild-type and α-CGRP-deficient mice (n = 4–6). #$P < 0.05$ compared with saline groups.

Table 1. *Total cell counts and cell fractions in BALF*

	Total Cell Counts, $\times 10^5$	Macrophages, %	Lymphocytes, %	Eosinophils, %	Polymorphonuclear Neutrophils, %
Saline					
+/+	1.04 ± 0.05	94.5 ± 0.3	5.1 ± 0.4	0.1 ± 0.1	0.3 ± 0.3
−/−	1.01 ± 0.07	94.8 ± 0.3	4.9 ± 0.3	0.1 ± 0.1	0.3 ± 0.3
Ovalbumin					
+/+	5.83 ± 1.26*	64.3 ± 9.7 *	3.5 ± 0.4	31.5 ± 10.0*	0.8 ± 0.2
−/−	5.84 ± 0.61*	62.9 ± 10.7*	3.7 ± 0.8	32.7 ± 11.0*	0.8 ± 0.3

Values are means ± SE. BALF, bronchoalveolar lavage fluid. *$P < 0.05$ compared to saline groups.

Meanwhile, $LTC_4/D_4/E_4$ was reduced to the same level in antigen-treated *CGRP*$^{-/-}$ mice and the saline-treated groups.

There were no differences in BALF ET-1 among the groups: 1.35 ± 0.32 and 1.01 ± 0.11 pg in saline-treated *α-CGRP*$^{+/+}$ and *α-CGRP*$^{-/-}$, respectively, and 2.03 ± 0.38 and 2.70 ± 0.60 pg in OA-treated *α-CGRP*$^{+/+}$ and *α-CGRP*$^{-/-}$, respectively.

Assessment of CGRP immunoreactivity. Figure 6 demonstrates the immunohistochemistry of CGRP in large airways. In the OA-sensitized wild-type mouse, significant immunoreactivity for CGRP was observed in the airway epithelium and submucosa, while the immunostaining was modest in the saline-treated wild-type animal. On the other hand, there was little CGRP immunoreactivity in saline- or OA-treated *α-CGRP*$^{-/-}$ mice. In small airways and lung parenchyma, little CGRP immunoreactivity was observed in each experimental group (Fig. 7). Table 2 summarizes the visual assessment of CGRP immunoreactivity in each group. In airway epithelium, submucosa, and smooth muscle of large airways, the scores were significantly higher in OA-treated *CGRP*$^{+/+}$ mice than in any other group, although there were marked differences between *α-CGRP*$^{+/+}$ and *α-CGRP*$^{-/-}$ mice. Meanwhile, the scores were much lower in peripheral airways and lung parenchyma than in large airways in the wild-type mice.

DISCUSSION

The results of the present experiments show that antigen-induced bronchial hyperresponsiveness was significantly reduced in CGRP-deficient mice. Meanwhile, eosinophil infiltration elicited by antigen challenge was unaffected by disruption of the CGRP gene. Antigen-induced increases in BALF $LTC_4/D_4/E_4$ were significantly attenuated in α-CGRP-disrupted mice. These findings suggest that CGRP could be involved in the antigen-induced airway hyperresponsiveness, but not eosinophil infiltration, in mice.

CGRP has pleiotropic and pathophysiological effects on various cells and organs (3, 44). CGRP exerts trophic effects on skeletal muscle and vascular smooth muscle (3). CGRP also modulates some macrophage functions, including antigen presentation (13, 36). In the respiratory system, CGRP is synthesized by sensory C-fibers in the respiratory tree (47). However, the pathophysiological roles of CGRP in the lung have not been determined. Palmer et al. (39) demonstrated that CGRP potently constricts human airway smooth muscle. On the other hand, recent studies have reported that CGRP acts as a potent inhibitor of responses elicited by bronchoconstrictive stimuli (4, 33). Regarding eosinophil chemotaxis, Numao and Agrawal (37) reported that neuropeptides, including CGRP, may play a significant role in eosinophil infiltration by priming cells in allergic inflammation. Meanwhile, Teixeira et al. (46) demonstrated that CGRP has little effect on eosinophil accumulation in guinea pig skin. In the present study, we hypothesized that CGRP could

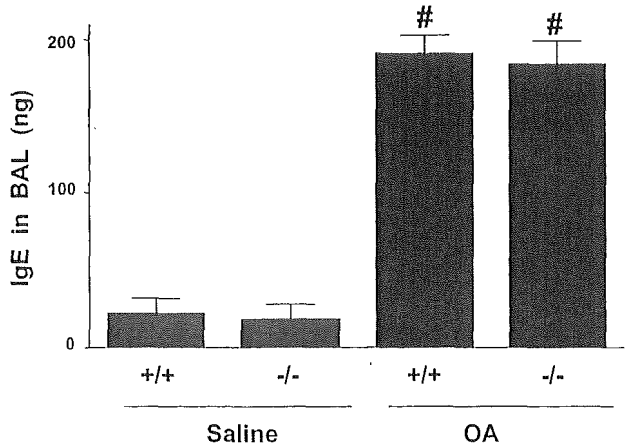

Fig. 4. IgE levels in BAL fluid in wild-type and α-CGRP-deficient mice (n = 4–6). #$P < 0.05$ compared with saline groups.

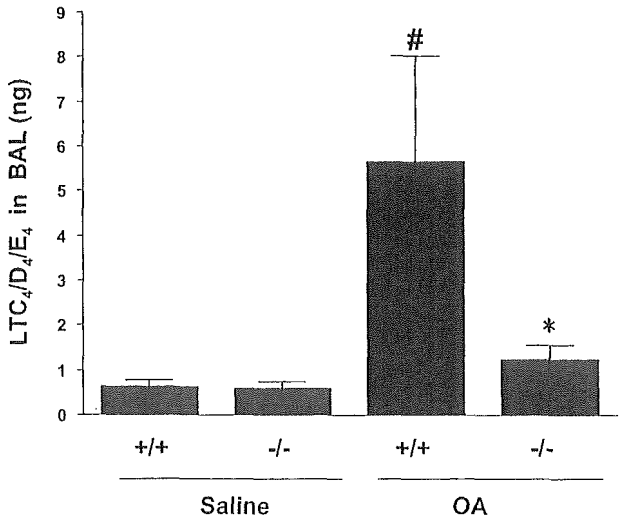

Fig. 5. Leukotriene (LT) $C_4/D_4/E_4$ levels in BAL fluid in wild-type and α-CGRP-deficient mice (n = 4–6). *$P < 0.05$ compared with sensitized wild-type mice. #$P < 0.05$ compared with saline groups.

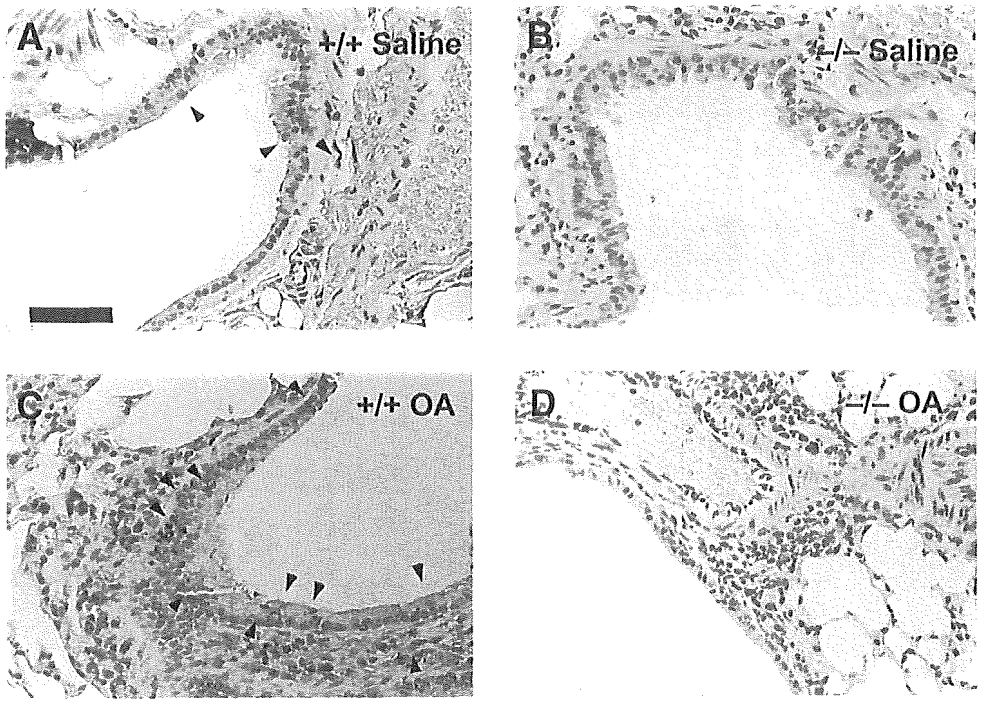

Fig. 6. Photomicrographs of CGRP immunohistochemical staining in large airways from saline-treated wild-type (*A*), saline-treated α-CGRP-deficient (*B*), OA antigen-treated wild-type (*C*), and OA antigen-treated α-CGRP-deficient (*D*) mice. Arrowheads, CGRP immunoreactivity. Immunoreactivity for CGRP was increased in antigen-treated wild-type mice (*C*) compared with unsensitized control (*A*). There was little immunostaining for CGRP in α-CGRP-deficient mice (*B* and *D*). Specimens were counterstained with hematoxylin. Scale bar, 50 μm.

play a significant role in the underlying mechanism of asthma. To test this hypothesis, we studied the allergic pulmonary responses using α-CGRP gene-disrupted mice, which have been recently established by Ohhashi et al. (38).

Allergen-induced airway hyperresponsiveness was significantly attenuated in the α-CGRP-deficient mice, suggesting that the existence of CGRP per se might be associated with bronchial hyperresponsiveness, which is a major trait of asthma (11, 12, 23). To our knowledge, this is the first report to use mutant mice to study whether the CGRP gene and endogenous CGRP could be involved in the airway hyperresponsiveness. Recently, using a pharmacological approach, Dakhama et al. (6) found that exogenous administration of CGRP to sensitized and challenged mice results in the normalization of airway responsiveness. However, the exact mechanism to explain the involvement of CGRP in airway hyperresponsiveness remains to be clarified. In the present study, the molecular and pathophysiologi-

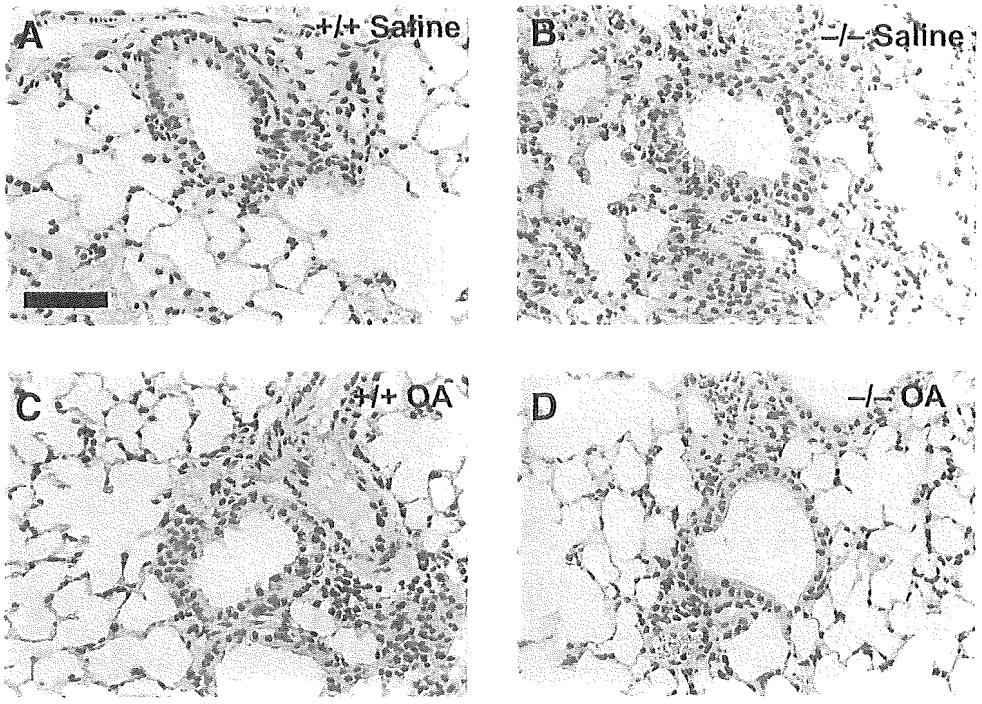

Fig. 7. Photomicrographs of CGRP immunohistochemical staining in small airways and lung parenchyma from saline-treated wild-type (*A*), saline-treated α-CGRP-deficient (*B*), OA antigen-treated wild-type (*C*), and OA antigen-treated α-CGRP-deficient (*D*) mice. There was little immunostaining for CGRP in each group. Specimens were counterstained with hematoxylin. Scale bar, 50 μm.

Table 2. *Visual assessment of airway CGRP immunoreactivity using immunoreactivity scores*

	Large Airways				
	Epithelium	Submucosa	Smooth muscle	Small Airways	Lung Parenchyma
Saline					
+/+	1.4 ± 0.2	1.4 ± 0.2	0.8 ± 0.1	0.4 ± 0.2	0.0 ± 0.0
−/−	0.2 ± 0.2*	0.2 ± 0.2*	0.0 ± 0.0*	0.0 ± 0.0*	0.0 ± 0.0
Ovalbumin					
+/+	2.6 ± 0.2†	2.4 ± 0.2†	2.1 ± 0.1†	0.4 ± 0.2	0.2 ± 0.2
−/−	0.2 ± 0.2*	0.4 ± 0.2*	0.1 ± 0.1*	0.0 ± 0.0*	0.0 ± 0.0

Values are means ± SE. CGRP, calcitonin gene-related peptide. *$P < 0.05$ compared with wild-type (+/+) groups. †$P < 0.05$ compared with saline groups.

cal mechanisms underlying airway hyperresponsiveness were further examined using CGRP-mutant mice.

One of the possible mechanisms is that CGRP and CGRP gene expression might affect airway inflammation, including eosinophilia, after antigen challenge. Airway eosinophilia is one of the common features in asthmatic patients and could be involved in bronchial hyperresponsiveness (11, 23). In the present study, however, no significant difference in BALF eosinophil counts was observed between the wild-type and CGRP-deficient mice. These results suggest that disruption of the CGRP gene has little effect on antigen-induced airway eosinophilia in mice. Although the sequence of rodent CGRP contains the tetrapeptide eosinophil chemotactic factor, the effect of CGRP on airway eosinophil infiltration is not remarkable in the present model. Therefore, CGRP-dependent airway hyperresponsiveness might not be mediated by eosinophilia.

Possibly, immunization provoked by antigen challenge might be affected by modulation of the CGRP gene. However, increased IgE levels after antigen challenge were observed in both groups, whereas there were no significant differences in measured IgE levels between the wild-type and CGRP-deficient groups. Alveolar protein leakage or airway mucus secretion assessed by BALF protein was consistent with the results of IgE measurement in this study. These findings indicate that modulation of the CGRP gene might not affect the mechanism of IgE production.

Recently, it has been shown that bronchial asthma is related to the generation of various potent mediators, including thromboxane, leukotriene, and ET-1 (28, 45, 49). These mediators are reported to be involved in airway hyperresponsiveness (28). Cysteinyl leukotrienes (LTC_4, LTD_4, and LTE_4) are reported to be among the most important targets for treating bronchial asthma. It has been shown that administration of cysteinyl leukotriene antagonist reduces antigen-induced airway hyperresponsiveness (10, 49) and the increases in airway smooth muscle after antigen exposure (49). Irvin et al. (14) demonstrated that antigen-induced airway hyperresponsiveness is significantly decreased in 5-lipoxygenase-deficient mice, suggesting the important role of leukotrienes in development of airway hyperresponsiveness. The potential sources of cysteinyl leukotrienes in the lung include alveolar macrophages, eosinophils, basophils, mast cells, and platelets (40). The proinflammatory activities of cysteinyl leukotrienes, including bronchoconstriction, mucus secretion, and plasma exudation, are mediated via the interaction with its receptor, the $CysLT_1$ receptor (9). In humans, it has been recently demonstrated that the $CysLT_1$ receptor is expressed in lung smooth muscle, lung macrophages, and peripheral blood leukocytes, while the identification of the $CysLT_1$ receptor is consistent with the anti-inflammatory actions of $CysLT_1$ receptor antagonists (9).

Potentially, genetic disruption of the CGRP gene may modulate the production levels of various potent mediators. We therefore measured possible mediators in the BALF and found that the production of cysteinyl leukotrienes was enhanced in the sensitized wild-type mice. In contrast, the level of cysteinyl leukotrienes was significantly reduced in the sensitized CGRP-deficient mice. There were no significant differences in thromboxane or ET-1 in each group. These observations indicate that CGRP gene disruption might inhibit the production of cysteinyl leukotrienes, which could be associated with reduced airway hyperresponsiveness. Meanwhile, after antigen challenge of wild-type and CGRP-deficient mice, there were no significant differences in the number of alveolar macrophages or eosinophils, i.e., potential sources of cysteinyl leukotrienes. One of the possible mechanisms to explain this observation is that CGRP might be involved in activation of the 5-lipoxygenase pathway.

In the present study, we used mutant mice deficient in α-CGRP but not β-CGRP. Therefore, these mutant mice should express β-CGRP. Because the α-CGRP antibody used in this study cross-reacts with β-CGRP (79%), the CGRP immunoreactivity represents α-CGRP and, similarly, β-CGRP. The very small amounts of CGRP immunoreactivity in the mutant mice may indicate β-CGRP expression in the lung. It has been previously reported that α-CGRP concentrations are approximately four times greater than β-CGRP concentrations in the rat lung, whereas in the intestine, β-CGRP concentrations are up to seven times greater than α-CGRP concentrations (26). Presumably, it seems that β-CGRP expression in the lung might not be affected by disruption of the α-CGRP gene in mice.

In the wild-type mice, we observed substantial CGRP immunoreactivity in the epithelium and submucosal tissues in large airways but not in small airways or parenchyma. Presumably, CGRP-immunoreactive

cells and tissues include nerve fibers in submucosal tissues, whereas airway epithelium contains nerves and NEBs. Terada et al. (47) reported that nerve plexuses of CGRP-immunoreactive fibers are located in the basal part of the rat tracheal epithelium. These CGRP-immunoreactive intraepithelial nerves lack myelin and Schwann sheaths and run through the bases of the epithelial cells (47). In this study, the CGRP immunoreactivity in large airway epithelium was remarkable, and it was enhanced by antigen challenge. These observations suggest that the epithelium of central airways, including nerves and NEBs, may have a significant role in antigen-induced airway hyperresponsiveness. Meanwhile, it is assumed that the contribution of peripheral airways and parenchyma to CGRP-related airway physiology is small.

Recently, Dakhama et al. (6) showed that CGRP expression was diminished in airway epithelium and submucosal nerve plexuses only after the third OA challenge, although CGRP depletion did not occur after the single antigen exposure. In our study, however, the single antigen challenge enhanced CGRP immunoreactivity in large airways in the wild-type mice, whereas little CGRP immunoreactivity was observed in CGRP-deficient mice in the absence or presence of antigen challenge. The present findings suggest that endogenous CGRP per se may be related to the development of antigen-induced airway hyperresponsiveness.

Genetic features, including single-nucleotide polymorphism, are potentially associated with the etiology of asthma. On the basis of the inheritance pattern, a number of genes could have substantial roles in the pathogenesis of bronchial asthma (43). Murine models of asthma have been recently used to investigate individual genes associated with airway hyperresponsiveness (8, 15, 16, 18, 31, 48). Because CGRP is one of the potent mediators possibly involved in bronchial asthma (39), genes regulating the function of CGRP, calcitonin receptor-like receptor, and RAMP1 could be targets to study the pathogenesis of asthma. Consistently, the present observations suggest that α-CGRP and the α-CGRP gene play significant roles in the molecular mechanism underlying bronchial asthma, indicating that the α-CGRP gene could be a target for single-nucleotide polymorphism research. The α-CGRP-mutant mice used in this study may contribute to the study of the genetic roles of α-CGRP in bronchial asthma and may provide novel insights into the pathophysiological roles of α-CGRP and the α-CGRP gene in vivo.

In summary, reduction of antigen-induced airway hyperresponsiveness was detected in α-CGRP-deficient mice. Meanwhile, eosinophilic infiltration associated with antigen exposure was not altered by disruption of the α-CGRP gene. Antigen-induced increases in cysteinyl leukotriene production were significantly reduced in α-CGRP-disrupted mice. Disruption of the α-CGRP gene might inhibit production of cysteinyl leukotrienes, which could be associated with reduced airway hyperresponsiveness. Antigen challenge enhanced CGRP immunoreactivity in the wild-type mice, whereas little CGRP immunoreactivity in epithelium or submucosa was observed in α-CGRP-deficient mice. These findings suggest that endogenous CGRP may be involved in development of antigen-induced airway hyperresponsiveness. Taken together, CGRP and CGRP gene expression might be involved in the pathogenesis of bronchial asthma by acting as a mediator. The CGRP-mutant mice may provide appropriate models to study molecular and pathophysiological mechanisms underlying diseases related to CGRP.

We thank Y. Tateno (University of Tokyo) for technical assistance.
This work was supported in part by a Grant-in-Aid for Scientific Research from the Ministry of Education, Science, Sports, and Culture, Japan, and an AstraZeneca research grant.

REFERENCES

1. **Amara SG, Arriza JL, Leff SE, Swanson LW, Evans RM, and Rosenfeld MG.** Expression in brain of a messenger RNA encoding a novel neuropeptide homologous to calcitonin gene-related peptide. *Science* 229: 1094–1097, 1985.
2. **Amara SG, Jonas V, Rosenfeld MG, Ong ES, and Evans RM.** Alternative RNA processing in calcitonin gene expression generates mRNAs encoding different polypeptide products. *Nature* 298: 240–244, 1982.
3. **Brain SD, Williams TJ, Tippins JR, Morris HR, and MacIntyre I.** Calcitonin gene-related peptide is a potent vasodilator. *Nature* 313: 54–56, 1985.
4. **Cadieux A, Monast NP, Pomerleau F, Fournier A, and Lanoue C.** Bronchoprotector properties of calcitonin-gene related peptide in guinea pig and human airways. *Am J Respir Crit Care Med* 159: 235–243, 1999.
5. **Chanez P, Springall D, Vignola AM, Moradoghi-Hattvani A, Polak JM, Godard P, and Bousquet J.** Bronchial mucosal immunoreactivity of sensory neuropeptides in severe airway diseases. *Am J Respir Crit Care Med* 158: 985–990, 1998.
6. **Dakhama A, Kanehiro A, Makela MJ, Loader JE, Larsen GL, and Gelfand EW.** Regulation of airway hyperresponsiveness by calcitonin gene-related peptide in allergen sensitized and challenged mice. *Am J Respir Crit Care Med* 165: 1137–1144, 2002.
7. **Davies D, Medeiros MS, Keen J, Turner AJ, and Haynes LW.** Endopeptidase-24.11 cleaves a chemotactic factor from α-calcitonin gene-related peptide. *Biochem Pharmacol* 43: 1753–1756, 1992.
8. **DeSanctis GT, Merchant M, Beier DR, Dredge RD, Grobholz JK, Martin TR, Lander ES, and Drazen JM.** Quantitative locus analysis of airway hyperresponsiveness in A/J and C57BL/6J mice. *Nat Genet* 11: 150–154, 1995.
9. **Figueroa DJ, Breyer RM, Defoe SK, Kargman S, Daugherty BL, Waldburger K, Liu Q, Clements M, Zeng Z, O'Neill GP, Jones TR, Lynch KR, Austen CP, and Evans JF.** Expression of the cysteinyl leukotriene 1 receptor in normal human lung and peripheral blood leukocytes. *Am J Respir Crit Care Med* 163: 226–233, 2001.
10. **Herd CM, Donigi-Gale D, Shoupe TS, Burroughs DA, Yeadon M, and Page CP.** Effect of a 5-lipoxygenase inhibitor and leukotriene antagonist (PF 5901) on antigen-induced airway responses in neonatally immunized rabbits. *Br J Pharmacol* 112: 292–298, 1994.
11. **Hogg JC.** Pathology of asthma. *J Allergy Clin Immunol* 92: 1–5, 1993.
12. **Holgate ST.** The epidemic of allergy and asthma. *Nature* 402: B2–B4, 1999.
13. **Hosoi J, Murphy GF, Egan CL, Lerner EA, Grabbe S, Asahina A, and Granstein RD.** Regulation of Langerhans cell function by nerves containing calcitonin gene-related peptide. *Nature* 363: 159–163, 1993.

14. **Irvin CG, Tu YP, Sheller JR, and Funk CD.** 5-Lipoxygenase products are necessary for ovalbumin-induced airway responsiveness in mice. *Am J Physiol Lung Cell Mol Physiol* 272: L1053–L1058, 1997.
15. **Ishii S, Kuwaki T, Nagase T, Maki K, Tashiro F, Sunaga S, Cao WH, Kume K, Fukuchi Y, Ikuta K, Miyazaki J, Kumada M, and Shimizu T.** Impaired anaphylactic responses but intact sensitivity to endotoxin in mice lacking a platelet-activating factor receptor. *J Exp Med* 187: 1779–1788, 1998.
16. **Ishii S, Nagase T, Tashiro F, Ikuta K, Sato S, Waga I, Kume K, Miyazaki J, and Shimizu T.** Bronchial hyperreactivity, increased endotoxin lethality and melanocytic tumorigenesis in transgenic mice overexpressing platelet-activating factor receptor. *EMBO J* 16: 133–142, 1997.
17. **Janssen PL and Tucker A.** Calcitonin gene-related peptide modulates pulmonary vascular reactivity in isolated rat lungs. *J Appl Physiol* 77: 142–146, 1994.
18. **Levitt RC and Mitzner W.** Autosomal recessive inheritance of airway hyperreactivity to 5-hydroxytryptamine. *J Appl Physiol* 67: 1125–1132, 1989.
19. **Lu B, Fu WM, Greengard P, and Poo MM.** Calcitonin gene-related peptide potentiates synaptic responses at developing neuromuscular junction. *Nature* 363: 76–79, 1993.
20. **Lundberg JM, Anders FC, Hua X, Hökfelt T, and Fischer JA.** Coexistence of substance P and calcitonin gene-related peptide-like immunoreactivities in sensory nerves in relation to cardiovascular and bronchoconstrictor effects of capsaicin. *Eur J Pharmacol* 108: 315–319, 1985.
21. **Mapp CE, Lucchini RE, Miotto D, Chitano P, Jovine L, Saetta M, Maestrelli P, Springall DR, Polak J, and Fabbri LM.** Immunization and challenge with toluene diisocyanate decrease tachykinin and calcitonin gene-related peptide immunoreactivity in guinea pig central airways. *Am J Respir Crit Care Med* 158: 263–269, 1998.
22. **McCormack D, Mak J, Coupe M, and Barnes PJ.** Calcitonin gene-related peptide vasodilation of human pulmonary vessels. *J Appl Physiol* 67: 1265–1270, 1989.
23. **McFadden ER and Gilbert IA.** Asthma. *N Engl J Med* 327: 1928–1937, 1992.
24. **McLatchie LM, Fraser NJ, Main MJ, Wise A, Brown J, Thompson N, Solary R, Lee MG, and Foord SM.** RAMPs regulate the transport and ligand specificity of the calcitonin-receptor-like receptor. *Nature* 393: 333–339, 1998.
25. **Merighi A, Polak JM, Gibson SJ, Gulbenkian S, Valentino KL, and Peirone SM.** Ultrastructural studies on calcitonin gene-related peptide-, tachykinin-, and somatostatin-immunoreactive neurons in rat dorsal root ganglia: evidence for the colocalization of different peptides in single secretory granules. *Cell Tissue Res* 254: 101–109, 1988.
26. **Mulderry PK, Ghatei MA, Spokes RA, Jones PM, Pierson AM, Hamid QA, Kanse S, Amara SG, Burrin JM, Legon S, Polak JM, and Bloom SR.** Differential expression of αCGRP and βCGRP by primary sensory neurons and enteric autonomic neurons of the rat. *Neuroscience* 25: 195–205, 1988.
27. **Nagase T, Fukuchi Y, Matsuse T, Sudo E, Matsui H, and Orimo H.** Antagonism of ICAM-1 attenuates airway and tissue responses to antigen in sensitized rats. *Am J Respir Crit Care Med* 151: 1244–1249, 1995.
28. **Nagase T, Ishii S, Katayama H, Fukuchi Y, Ouchi Y, and Shimizu T.** Airway responsiveness in transgenic mice overexpressing platelet-activating factor receptor: roles of thromboxanes and leukotrienes. *Am J Respir Crit Care Med* 156: 1621–1627, 1997.
29. **Nagase T, Ishii S, Kume K, Uozumi N, Izumi T, Ouchi Y, and Shimizu T.** Platelet-activating factor mediates acid-induced lung injury in genetically engineered mice. *J Clin Invest* 104: 1071–1076, 1999.
30. **Nagase T, Ishii S, Shindou H, Ouchi Y, and Shimizu T.** Airway hyperresponsiveness in transgenic mice overexpressing platelet-activating factor receptor is mediated by an atropine-sensitive pathway. *Am J Respir Crit Care Med* 165: 200–205, 2002.
31. **Nagase T, Kurihara H, Kurihara Y, Aoki T, Fukuchi Y, Yazaki Y, and Ouchi Y.** Airway hyperresponsiveness to methacholine in mutant mice deficient in endothelin-1. *Am J Respir Crit Care Med* 157: 560–564, 1998.
32. **Nagase T, Matsui H, Aoki T, Ouchi Y, and Fukuchi Y.** Lung tissue behaviour in the mouse during constriction induced by methacholine and endothelin-1. *J Appl Physiol* 81: 2373–2378, 1996.
33. **Nagase T, Ohga E, Katayama H, Sudo E, Aoki T, Matsuse T, Ouchi Y, and Fukuchi Y.** Roles of calcitonin-gene related peptide (CGRP) in hyperpnea-induced constriction in guinea pigs. *Am J Respir Crit Care Med* 154: 1551–1556, 1996.
34. **Nagase T, Uozumi N, Ishii S, Kita Y, Yamamoto H, Ohga E, Ouchi Y, and Shimizu T.** A pivotal role of cytosolic phospholipase A_2 in bleomycin-induced pulmonary fibrosis. *Nat Med* 8: 480–484, 2002.
35. **Nagase T, Uozumi N, Ishii S, Kume K, Izumi T, Ouchi Y, and Shimizu T.** Acute lung injury by sepsis and acid aspiration: a key role for cytosolic phospholipase A_2. *Nat Immunol* 1: 42–46, 2000.
36. **Nong YH, Titus RG, Ribeiro JMC, and Remold HG.** Peptides encoded by the calcitonin gene inhibit macrophage function. *J Immunol* 143: 45–49, 1989.
37. **Numao T and Agrawal DK.** Neuropeptides modulate human eosinophil chemotaxis. *J Immunol* 149: 3309–3315, 1992.
38. **Oh-hashi Y, Shindo T, Kurihara Y, Imai T, Wang Y, Morita H, Imai Y, Kayaba Y, Nishimatsu H, Suematsu Y, Hirata Y, Yazaki Y, Nagai R, Kuwaki T, and Kurihara H.** Elevated sympathetic nervous activity in mice deficient in αCGRP. *Circ Res* 89: 983–990, 2001.
39. **Palmer JBD, Cuss FMC, Mulderry PK, Ghatei MA, Springall DR, Cadieux A, Bloom SR, Polak JM, and Barnes PJ.** Calcitonin gene-related peptide is localized to human airway nerves and potently constricts human airway smooth muscle. *Br J Pharmacol* 91: 95–101, 1987.
40. **Penrose JF, Spector J, Baldasaro M, Xu K, Boyce J, Arm JP, Austen KF, and Lam BK.** Molecular cloning of the gene for human leukotriene C_4 synthase: organization, nucleotide sequence, and chromosomal localization to 5q35. *J Biol Chem* 271: 11356–11361, 1996.
41. **Pinto A, Sekizawa K, Yamaya M, Ohrui T, Jia YX, and Sasaki H.** Effects of adrenomedullin and calcitonin gene-related peptide on airway and pulmonary vascular smooth muscle in guinea-pigs. *Br J Pharmacol* 119: 1477–1483, 1996.
42. **Rosenfeld MG, Mermod JJ, Amara SG, Swanson LW, Sawchenko PE, Rivier J, Vale WW, and Evans RM.** Production of a novel neuropeptide encoded by the calcitonin gene via tissue-specific RNA processing. *Nature* 304: 129–135, 1983.
43. **Sandford A, Weir T, and Paré P.** The genetics of asthma. *Am J Respir Crit Care Med* 153: 1749–1765, 1996.
44. **Solway J and Leff AR.** Sensory neuropeptides and airway function. *J Appl Physiol* 71: 2077–2087, 1991.
45. **Springall DR, Howarth PH, Counihan H, Djukanovic R, Holgate ST, and Polak JM.** Endothelin immunoreactivity of airway epithelium in asthmatic patients. *Lancet* 337: 697–701, 1991.
46. **Teixeira MM, Williams TJ, and Hellewell PG.** E-type prostaglandins enhance local oedema formation and neutrophil accumulation but suppress eosinophil accumulation in guinea-pig skin. *Br J Pharmacol* 110: 416–422, 1993.
47. **Terada M, Iwanaga T, Iwanaga HT, and Adachi I.** Calcitonin gene-related peptide (CGRP)-immunoreactive nerves in the tracheal epithelium of rats: an immunohistochemical study by means of whole mount preparations. *Arch Histol Cytol* 55: 219–233, 1992.
48. **Uozumi N, Kume K, Nagase T, Nakatani N, Ishii S, Tashiro F, Komagata Y, Maki K, Ikuta K, Ouchi Y, Miyazaki J, and Shimizu T.** Role of cytosolic phospholipase A_2 in allergic response and parturition. *Nature* 390: 618–622, 1997.
49. **Wang CG, Du T, Xu LJ, and Martin JG.** Role of leukotriene D_4 in allergen-induced increases in airway smooth muscle in the rat. *Am Rev Respir Dis* 148: 413–417, 1993.

Identification of Multiple Novel Epididymis-Specific β-Defensin Isoforms in Humans and Mice[1]

Yasuhiro Yamaguchi,*† Takahide Nagase,† Ryosuke Makita,* Shigetomo Fukuhara,* Tetsuji Tomita,† Takashi Tominaga,‡ Hiroki Kurihara,[2]* and Yasuyoshi Ouchi†

Defensins comprise a family of cationic antimicrobial peptides that are characterized by the presence of six conserved cysteine residues. We identified two novel human β-defensin (hBD) isoforms by mining the public human genomic sequences. The predicted peptides conserve the six-cysteine motif identical with hBD-4, termed hBD-5 and hBD-6. We also evaluated the characteristics of the mouse homologs of hBD-5, hBD-6, and HE2β1, termed mouse β-defensin (mBD)-12, mBD-11, and mouse EP2e (mEP2e). The mBD-12 synthetic peptide showed salt-dependent antimicrobial activity. We demonstrate the epididymis-specific expression pattern of hBD-5, hBD-6, mBD-11, mBD-12, and mEP2e. In situ hybridization revealed mBD-11, mBD-12, and mEP2e expression in the columnar epithelium of the caput epididymis, contrasting with the predominant expression of mBD-3 in the capsule or septum of the whole epididymis. In addition, the regional specificity of mBD-11, mBD-12, and mEP2e was somewhat overlapping, but not identical, in the caput epididymis, suggesting that specific regulation may work for each member of the β-defensin family. Our findings indicated that multiple β-defensin isoforms specifically and cooperatively contribute to the innate immunity of the urogenital system. *The Journal of Immunology,* **2002, 169: 2516–2523.**

Defensins are cationic antimicrobial peptides that include six specific cysteine residues and can be divided into the α- and β-defensin subfamilies. Three human α-defensins, human neutrophil peptides (HNP)[3]-1, -2, and -3, were isolated from human neutrophils and showed broad-spectrum microbicidal activity (1). The first mammalian β-defensin was discovered from the bovine respiratory tract, named tracheal antimicrobial peptide (2). Subsequently, lingual antimicrobial peptide was isolated from the bovine tongue (3).

Four human β-defensin (hBD) isoforms have been identified to date: hBD-1, -2, -3, and -4 (4–7). HE2β1, identified as one major splicing variant of the human EP2 gene, also contains the specific cysteine motif (8–11). All hBDs show potent antimicrobial activity, especially against Gram-negative bacteria, whereas the function of HE2β1 had not been confirmed (5–7, 12–14). In mice, mouse β-defensin (mBD)-1, -2, -3, -4, -5, -6, -7, -8, -9, -11, -13, and -35 have been identified at the National Center for Biotechnology Information (NCBI) gene bank, although the characteristics of mBD-5, mBD-9, mBD-11, mBD-13, and mBD-35 have not been published (15–21). mBD-1 and mBD-3 are regarded as mouse homologs of hBD-1 and hBD-2, respectively, and also showed antimicrobial activity (16, 18). hBD-1, hBD-2, and hBD-3 showed the widespread distribution in various organs like urogenital tissues, skin, respiratory tracts, intestinal tracts, testis, and placenta (22–26). Although the tissue distribution of mBD-5, mBD-7, mBD-8, mBD-9, mBD-11, mBD-13, and mBD-35 have not been evaluated in mice, the other known mBD isoforms also show the expression in multiple tissues, such as kidney, esophagus, tongue, trachea, and skeletal muscle (15–20).

Furthermore, the novel antimicrobial peptide Bin1b was identified in the rat epididymis and its putative amino acid sequence is included the conserved six-cysteine motif (27). Bin1b is partially homologous with HE2β1 and more homologous with the chimpanzee epididymal protein EP2E in its amino acid sequence (28). Interestingly, Bin1b showed no expression in the other major organs, such as the lung or kidney. Subsequently, hBD-4 cDNA was identified and its expression was also almost confined to the testis with much lower expression in the gastric antrum (7). These two isoforms are unique in their confined expression pattern.

Because the defensin genes comprise a large gene cluster in chromosome 8, the genomic sequence is useful to identify novel defensin genes (11, 29, 30). Recent reports indicate the presence of >25 human or mouse genes that could be encoding β-defensin peptide, although the characteristics of these genes have not been evaluated well (31). In this work we report the peculiar characteristics of multiple epididymis-specific β-defensin isoforms in humans and mice, including two novel hBD isoforms, named hBD-5 and hBD-6, and two novel mBD isoforms, named mBD-12 and mouse EP2e (mEP2e), respectively.

Materials and Methods

Cloning of hBD-5 and hBD-6 cDNA

We obtained the nucleotide sequence of the human genome around the β-defensin gene cluster in chromosome 8 from the NCBI public database (NT_019483). This sequence was translated in all six possible reading frames and was searched for the specific cysteine pattern; multiple possible

*Division of Integrative Cell Biology, Department of Embryogenesis, Institute of Molecular Embryology and Genetics, Kumamoto University, Kumamoto, Japan; and †Department of Geriatric Medicine, Graduate School of Medicine, University of Tokyo, and ‡Department of Urology, Mitsui Memorial Hospital, Tokyo, Japan

Received for publication April 1, 2002. Accepted for publication June 28, 2002.

The costs of publication of this article were defrayed in part by the payment of page charges. This article must therefore be hereby marked *advertisement* in accordance with 18 U.S.C. Section 1734 solely to indicate this fact.

[1] This work was supported by the Japan Society for the Promotion of Science Research for the Future Program; a Research Grant for Cardiovascular Diseases (11C-1) from the Ministry of Health and Welfare; the Program for Promotion of Fundamental Studies in Health Sciences of the Organization for Pharmaceutical Safety and Research (to H.K.); Grants-in-Aid for Scientific Research from the Ministry of Education, Science and Culture, Japan (to H.K., T.N., and Y.Y.), the Yamanouchi Foundation for Research on Metabolic Disorders, and the Novartis Foundation for Gerontological Research (to T.N.).

[2] Address correspondence and reprint requests to Dr. Hiroki Kurihara, Division of Integrative Cell Biology, Department of Embryogenesis, Institute of Molecular Embryology and Genetics, Kumamoto University, 2-2-1 Honjo, Kumamoto-shi, Kumamoto 860-0811, Japan. E-mail address: kurihara@kaiju.medic.kumamoto-u.ac.jp

[3] Abbreviations used in this paper: HNP, human neutrophil peptide; hBD, human β-defensin; mBD, mouse β-defensin; mEP2e, mouse EP2e; EST, expressed sequence tag.

0022-1767/02/$02.00

β-defensin genes were obtained. We used the basic local alignment search tool against the expressed sequence tag (EST) database and obtained a sequence identical with the DEFB6 gene (31). Based on this EST sequence (AW103145, AI910580) and the corresponding genomic sequence, we designed a pair of specific intron-spanning primers for RT-PCR (forward primer, 5′-CAGTCATGAGGACTTTCCTC-3′; reverse primer, 5′-AGA AGCTAGGTTATGTATGC-3′). Reverse transcription was performed on total human epididymis/testis RNA (Clontech Laboratories, Palo Alto, CA) using Superscript II. The PCR conditions were 94°C for 40 s, 60°C for 30 s, and 72°C for 1 min conducted for 35 cycles.

In addition, we designed two specific primers for RT-PCR based on the genomic sequence of the DEFB5 gene (forward primer, 5′-GTCGTG CAAGCTTGGTCGGG-3′; reverse primer, 5′-CCAGGTCTGCTTCTA AGGCC-3′) (31). We performed RT-PCR to evaluate the expression of this gene as described above. Subsequently, we determined the 5′ end of this novel cDNA sequence using a 5′ RACE kit (Life Technologies, Rockville, MD) performed on total RNA from the human epididymis.

Cloning of the mouse homologs of hBD-5, hBD-6, and HE2β1

We screened the homologous sequence of the DEFB5 gene using the basic local alignment search tool at NCBI and obtained the published full-length cDNA sequence from the adult mouse epididymis (AK020311, RIKEN full-length enriched library; clone 9230103N16) (32).

To identify the homolog of HE2β1, we designed a pair of degenerate PCR primers from the amino acid sequences conserved between HE2β1 and Bin1b: forward primer, 5′-GAYRTACCACCKGGAATHAG-3′; reverse primer, 5′-GATACRCARCATCTRTTCCA-3′. RT-PCR was performed on adult mouse epididymis RNA. The PCR conditions were 94°C for 40 s, 60°C for 30 s, and 72°C for 1 min conducted for 35 cycles. The sequencing of the PCR products revealed the homologous fragment with Bin1b cDNA. We screened the EST library using this novel nucleotide sequence and obtained the full-length cDNA sequence (AK020333, RIKEN full-length enriched library; clone 9230111C08) (32).

We also obtained the partial mouse genomic sequence containing the mBD-35 gene from the NCBI database (AL590619). This sequence was translated in all six possible reading frames and detected the homologous genomic sequence with the hBD-6 gene. Based on this genomic sequence, we designed two specific intron-spanning primers to confirm the expression (forward primer, 5′-GCCCTTCAGGTCATGAAGAC-3′; reverse primer, 5′-AGCATCTGCTTCCATCAGGT-3′). RT-PCR was performed as described on the DEFB6 gene. To determine the full-length cDNA sequences of these three mBD isoforms, we used 5′-RACE and 3′-RACE kits on the mouse epididymis RNA (Life Technologies).

Analysis of the genomic organization

As for human genomic sequences and mBD-11 genomic sequences, we used the public sequences at NCBI. As for the mBD-12 and mEP2e genomic sequences, we designed a pair of specific PCR primers from mBD-12 (forward primer, 5′-TGAAGAATCTCCCCTCAAACATGG-3′; reverse primer, 5′-TTCACAAGGCAAAGTTACAG-3′) and mEP2e (forward primer, 5′-ATCAGTCACACCTGCTTTCC-3′; reverse primer, 5′-ATCCTTTCACCGGACCTTTG-3′). PCR was performed on the isolated mouse genomic DNA using the Advantage HF-2 PCR kit (Clontech Laboratories). The PCR products were cloned to pCR4-TOPO vector (Invitrogen, Carlsbad, CA) and the inserts were sequenced to determine the splicing site.

Synthesis of mBD-12 mature peptide

We synthesized chemically the putative mBD-12 mature peptide spanning 34 COOH-terminal amino acids of the precursor at the Peptide Institute (Minoh, Japan). The synthetic peptide was air-oxidated for three disulfide bonds. The material, eluted in a single peak on RP-HPLC and confirmed by mass spectroscopy, was lyophilized and dissolved in 0.01% acetic acid.

Analysis of antimicrobial activity

We followed the colony count assay described by Harwig et al. (33) with some modification. Mid-logarithmic-phase *Escherichia coli* (ATCC 25922 strain) was suspended in 10 mM sodium phosphate buffer to adjust the density to 5×10^7 CFU/ml, and this suspension was mixed with mBD-12 solution. The final sodium concentration of this mixture was 15 mM, and the mBD-12 concentration was adjusted to 2, 20, or 200 μg/ml. As a control, the mixture without mBD-12 was also incubated. After a 2-h incubation of these mixtures at 37°C, the 10-fold serial dilutions were spread over tripticase soy agar plates and incubated at 37°C for 48 h. After counting the numbers of colonies on the plates, we calculated ratios of survived-to-control colony numbers as survival ratios.

The salt sensitivity of the antimicrobial activity was also evaluated. We adjusted the final sodium concentration of the bacterial mixture to 15, 50, 100, or 150 mM with NaCl and incubated the mixture for 2 h with 20 μg/ml mBD-12. As a control, the mixture without mBD-12 was also incubated at each sodium concentration. After the 2-h incubation, the 10-fold serial dilutions were spread over the plates and incubated for 48 h as described above. The procedures were repeated more than four times at each sodium concentration.

RT-PCR

Human epididymis and testis were obtained from the surgical samples of a prostate cancer patient in Mitsui Memorial Hospital (Tokyo, Japan). The institutional review board of Mitsui Memorial Hospital approved this study. We isolated human RNA from these specimens using Isogen (Nippon Gene, Toyama, Japan). We also purchased human RNA of brain, liver, lung, trachea, kidney, heart, and skeletal muscle from Clontech Laboratories. Mouse RNA was isolated from the indicated organs of sexually mature male ICR mice using Isogen (Nippon Gene). A total of 5 μg of each sample was reverse-transcribed by random hexamer primers using Superscript II (Life Technologies).

We designed a pair of specific intron-spanning primers from hBD-5 (forward primer, 5′-TTGGTTCAACTGCCATCAGG-3′; reverse primer, 5′-CCAGGTCTGCTTCTAAGGCC-3′), hBD-4 (forward primer, 5′-CTC CGACTTGCGTCTGCTTC-3′; reverse primer, 5′-CCTGAGCAAAACTT TCGATC-3′), and HE2β1 (forward primer, 5′-TCTGGCTTGCAGT GCTCTTG-3′; reverse primer, 5′-CTTGGGATACTTCAACATCC-3′). As for mouse genes, we also designed a pair of specific intron-spanning primers from mBD-12 (forward primer, 5′-TGAAGAATCTCCCCT CAAACATGG-3′; reverse primer, 5′-GGAGCATAGCACTTTCGTTTG-3′), mEP2e (forward primer, 5′-ATCAGTCACACCTGCTTTCC-3′; reverse primer, 5′-CACATACTCAAAGCCTTTGG-3′), and mBD-3 (forward primer, 5′-GCTTCAGTCATGAGGATCCATTACCTTC-3′; reverse primer, 5′-GCTAGGGAGCACTTGTTTGCATTTAATC-3′). PCR was performed on 0.5 μl of reverse transcriptase reaction for a total volume of 25 μl using *Taq* polymerase (Takara Shuzo, Otsu, Japan). The PCR conditions were 94°C for 40 s, 60°C for 30 s, and 72°C for 1 min conducted for the indicated cycles. Amplification of G3PDH was also performed in parallel as a control.

In situ hybridization

A 290-bp fragment of mBD-11 cDNA, a 700-bp fragment of mBD-12 cDNA, and a 340-bp fragment of mEP2e cDNA were isolated from the mouse epididymis RNA as described above. We also isolated a 300-bp fragment containing mBD-3 exon 2 from bacterial artificial chromosome D11 (Incyte Genomics, Palo Alto, CA) by PCR amplification. Antisense and sense RNA probes were prepared from these fragments by T3 or T7 RNA polymerase using a DIG RNA labeling kit (Roche, Basel, Switzerland).

The mouse epididymis was fixed in 4% paraformaldehyde at 4°C overnight and was cryosectioned at 20 μm. The sections were treated with 1 μg/ml proteinase K for 5 min at 37°C and 2 mg/ml glycine for 30 s, postfixed in 3.7% formaldehyde in PBS for 20 min, and acetylated with 0.25% acetic anhydride in 0.1 M triethanolamine for 10 min. Hybridization with DIG-labeled probe was conducted overnight at 55°C in 5× SSC, 1% SDS, 50% formamide, and 1 mg/ml yeast tRNA containing 1 mg/ml probe. Then, the sections were washed twice in 2× SSC, 1% SDS, 50% formamide and once in 0.2× SSC, 0.1% SDS, 50% formamide at 60°C for 30 min each. The sections were incubated with anti-DIG alkaline phosphatase-conjugated Abs diluted 1/2000 with 100 mM maleic acid (pH 7.5), 50 mM NaCl, 0.1% Tween 20 overnight at 4°C, followed by an alkaline phosphatase reaction step under the following conditions: 50 mg/ml nitroblue tetrazolium chloride, 50 mg/ml 5-bromo-4-chloro-3-indolyl phosphate, 10% (w/v) polyvinylalcohol, 100 mM Tris-Cl (pH 9.5), 50 mM $MgCl_2$, 100 mM NaCl, 0.1% Tween 20. The sections were developed at 37°C in the dark.

Results

Identification of two novel hBD genes

Based on the public human genomic sequence (NT_019483), we identified multiple sequences that could be encoding β-defensin peptide because of its predicted cysteine pattern. We confirmed the existence of two corresponding transcripts of these putative genes by RT-PCR. The predicted amino acid sequences of these novel transcripts contained the specific six-cysteine motif identical with hBD-4 and we named these novel peptides hBD-5 and hBD-6, although the

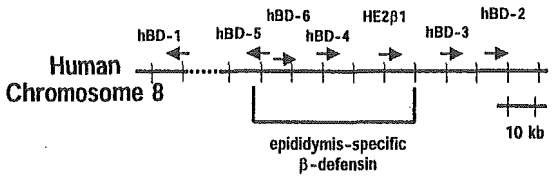

FIGURE 1. Schematic view of the hBD gene cluster on chromosome 8. The arrows indicate the direction of transcription of the indicated β-defensin isoforms. The epididymis-specific genes were located in the adjacent regions.

transcription initiation site of hBD-6 cDNA has not been determined, probably due to a too-low amount of hBD-6 mRNA.

The hBD-5 gene was located ~74.4 kb from the hBD-2 gene and ~19 kb from the hBD-4 gene (Fig. 1). The hBD-5 gene encoded its transcript in the antisense direction to the hBD-2, -3, -4, and HE2β1 genes. The hBD-6 gene was located between the hBD-4 and hBD-5 genes. hBD-5 contained three exons separated by the first 343-bp intron and the second 1248-bp intron while hBD-6 contained two exons separated by a 3575-bp intron (Fig. 2). No NF-κB consensus sites were found within the 5-kb promoter of the hBD-5 gene. The hBD-6 gene contains the NF-κB consensus sequence (GGGRNTYC) 5 and 1.3 kbp upstream of the start codon like the hBD-2 gene, which contains multiple NF-κB binding sites (29, 34).

Identification of the mouse homolog of hBD-5, hBD-6, and HE2β1

RIKEN's full-length cDNA sequence from the adult mouse epididymis (AK020311) exhibited ~77% identity with the hBD-5 coding region. We also confirmed the transcript using RT-PCR, 5′-RACE, and 3′-RACE on the mouse epididymis RNA. Our sequence analysis contained a 2-nt difference from RIKEN's sequence in the 3′ noncoding region. Because this mouse homolog corresponded to the Defb12 genomic sequence indicated by Schutte et al. (31), we named this isoform mBD-12. The genomic sequencing revealed that the mBD-12 gene was also separated by one short intron and one relatively long intron like hBD-5. The nucleotide sequence of the mBD-12 exon 3 coding region was 97.4% identical (191 of 196) with the corresponding sequence of mBD-35 cDNA (AJ437650) in the NCBI database, although mBD-12 exon 1 and exon 2 showed no homology with mBD-35. The genomic sequence of the second mBD-12 intron was also quite different from the mBD-35 genomic sequence, indicating that different genes encode these transcripts.

A hBD-5 gene

```
attcacttcacggatcaagagcatctccccattacttttaaataaaaat
gagcctctcatttgggtcttctc      AAGGAAATCCCAATCTCTATTC
CGAAGAGTCTTCCCTAAAAGATGGCCCTGATCAGGAAGACATTTTATTTT
                       M  A  L  I  R  K  T  F  Y  F
CTATTTGCTATGTTCTTCATTTTGGTTCAACTGCCATCAG   gtaagtaa
 L  F  A  M  F  F  I  L  V  Q  L  P  S
aaatgg
                  ·····343 bp ·····.
                                                ttgttttt
gaatttag  GGTGCCAGGCAGGACTTGATTTTTCCCAACCATTTCCATC
          G  C  Q  A  G  L  D  F  S  Q  P  F  P  S
AG  gtaagtta
                  ·····1248 bp ·····.
                                                tggcacag  GT
                                                          G
GAGTTTGCTGTCTGTGAGTCGTGCAAGCTTGGTCGGGGAAAATGCAGGAA
 E  F  A  V  C  E  S  C  K  L  G  R  G  K  C  R  K
GGAGTGCTTGGAGAATGAGAAGCCCGATGGAAATTGCAGGCTGAACTTTC
   E  C  L  E  N  E  K  P  D  G  N  C  R  L  N  F
TCTGCTGCAGACAGAGGATCTGACAAACCAGACCAGCACACTTCT·····.
L  C  C  R  Q  R  I  *
```

B hBD-6 gene

```
···ATGAGGACTTTCCTCTTTCTCTTTGCCGTGCTCTTCTTTCTGACCCCAG
   M  R  T  F  L  F  L  F  A  V  L  F  F  L  T  P
gtaaaatgggcat
                  ····· 3575 bp ·····.
                                                ttccctcgtgtag
CCAAGAATGCATTTTTTGATGAGAAATGCAACAAACTTA'AAGGGACATGC
A  K  N  A  F  F  D  E  K  C  N  K  L  K  G  T  C
AAGAACAATTGCGGGAAAAATGAAGAACTTATTGCTCTCTGCCAGAAGTC
 K  N  N  C  G  K  N  E  E  L  I  A  L  C  Q  K  S
TCTGAAATGCTGTCGGACCATCCAGCCATGTGGGAGCATTATAGATTAAT
   L  K  C  C  R  T  I  Q  P  C  G  S  I  I  D  *
GCAGAAGATTTAGGTTTCCAGAGAAGCATACATAACCTAG···.
```

FIGURE 2. Nucleotide and amino acid sequences of hBD-5 (*A*) and hBD-6 (*B*). Exon sequences are shown in capital letters. The exon-intron splice site sequences conform to the consensus rule. The dashed underlining indicates a TATA box-like sequence of the hBD-5 promoter. The boxes indicate the specific cysteine residues identical with hBD-4 and the dashed boxes indicate the additional cysteine residues unique to hBD-5, hBD-6, and their mouse homologs.

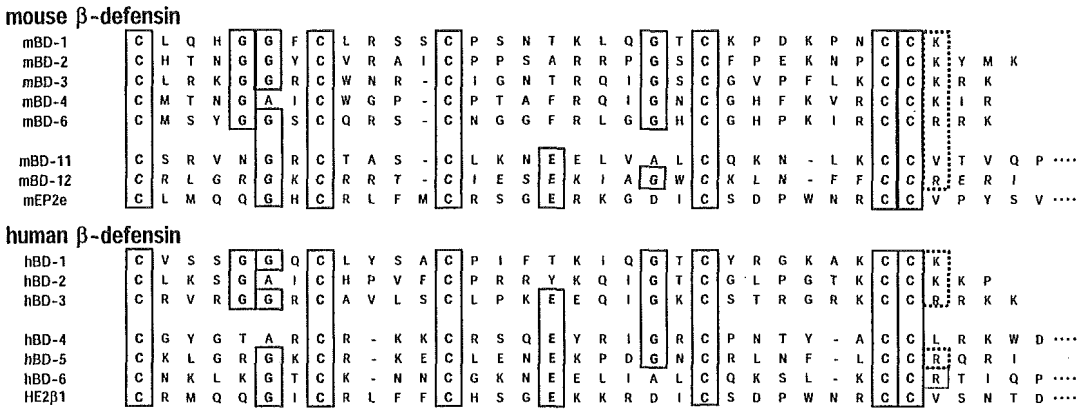

FIGURE 3. Comparison of the predicted amino acid sequences of the hBD and mBD families. Shown are partial amino acid sequences of the hBD and mBD isoforms whose tissue distribution was evaluated. The isoforms below the space were included in the epididymis-specific β-defensin subgroup. The solid boxes indicate the conserved residues among the multiple hBDs and mBDs. The dashed boxes show the conserved cationic residues.

Degenerate PCR amplification of the mouse epididymis cDNA with primers common to HE2β1 and Bin1b revealed a novel β-defensin sequence homologous with Bin1b. The cDNA sequence was identical with RIKEN's full-length cDNA sequence of the adult mouse epididymis (AK020333) (32). We also confirmed the corresponding transcript using RT-PCR, 5′-RACE, and 3′-RACE on the mouse epididymis RNA. The predicted amino acid sequence of this cDNA is 68.1% (47 of 69) identical with chimpanzee EP2E and 88.4% (61 of 69) identical with Bin1b, and we named this β-defensin isoform mEP2e. The genomic sequence revealed that the mEP2e gene was composed of only two exons separated by an ~1.2-kb intron, supporting mEP2e correspond to the EP2E splicing variant in the chimpanzee EP2 gene. The HE2β1 gene was composed of three exons separated by the first 583-bp intron and the second 11815-bp intron corresponding to the EP2D isoform (9–11, 28). The amino acid sequence encoded by the mEP2e exon 2 was also 67.3% (35 of 52) identical with the corresponding sequence of HE2β1. We could not detect the mouse variant corresponding to the EP2D isoform using the 5′-RACE system.

Using the public mouse nucleotide database at the NCBI (AL580619), we detected the genomic sequence homologous with the hBD-6 gene and confirmed the corresponding transcript using RT-PCR, 5′-RACE, and 3′-RACE on the mouse epididymis RNA. This mouse homolog was completely identical with defb11 gene at the NCBI database (AJ437648), named mBD-11. The predicted amino acid sequence of mBD-11 is 70.9% (46 of 65) identical with hBD-6 corresponding sequence. mBD-11 was composed of two exons separated by a 2567-bp intron like hBD-6. No NF-κB consensus sites were found within the 5-kb promoter of the mBD-12 gene.

Comparison of the hBD and mBD isoforms

In Fig. 3, we compared the partial amino acid sequences of hBD-5, hBD-6, mBD-11, mBD-12, and mEP2e with the known β-defensin isoforms whose tissue distribution had been evaluated. All the isoforms contain the specific cysteine motif (whose cysteine residues are referred to as C1, C2, C3, C4, C5, and C6 residues in order here).

Although the amino acid sequences were quite variable among the members of the β-defensin family, except the specific cysteine motif, there are some residues relatively conserved, such as the glycine two positions before the C2 residue (Fig. 3). As described below, mBD-11, mBD-12, and mEP2e in the mBD family and HE2β1, hBD-4, hBD-5, and hBD-6 in the hBD family showed the epididymis-specific expression pattern. These isoforms conserve the glutamic acid residue six positions before the C4 residue and do not conserve the glycine residue three positions before the C2 residue. These features are rather common among the potentially new β-defensin isoforms whose expression had not been established (33). Interestingly, α-defensin also includes the glutamic acid residue six positions before the C4 residue (1, 35).

Antimicrobial activity of synthetic mBD-12 peptide

To confirm the antimicrobial activity of mBD-12, we synthesized a putative mature peptide of mBD-12. The synthetic peptide

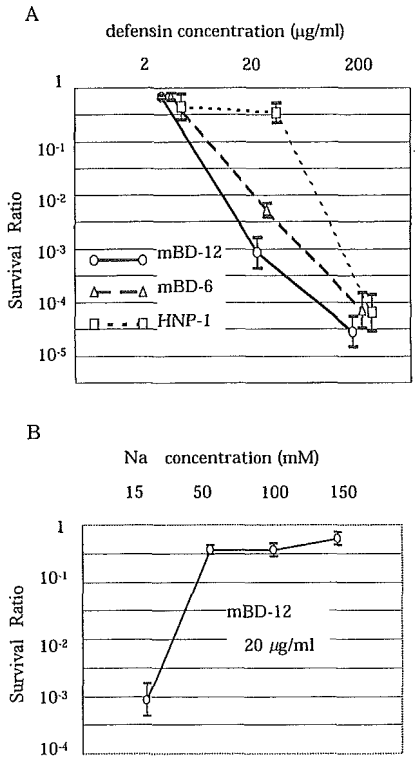

FIGURE 4. Antimicrobial activity of mBD-12 synthetic peptide. The survival ratio is the ratio of the number of survived colonies to that of control colonies. The means and the SEs of the $\log_{10}$ survival ratio are depicted. We also added the data of mBD-6 and HNP-1, which had been previously reported. *A*, mBD-12 showed significantly more potent microbicidal activity against *E. coli* at the concentration of 20 μg/ml than HNP-1 (Student's *t* test, $p < 0.01$). *B*, mBD-12 antimicrobial activity was significantly reduced at the environmental sodium concentrations of 50, 100, and 150 mM (Student's *t* test, $p < 0.01$).

showed bactericidal activity against *E. coli*. We compared the potency of mBD-12 with mBD-6 and HNP-1 synthetic peptide, whose data had been previously reported (20). mBD-12 bactericidal activity was significantly more potent than HNP-1 at the concentration of 20 μg/ml (Student's t test, $p < 0.01$) (Fig. 4*A*). This potency was comparable to other β-defensins because the minimum inhibitory concentration of recombinant mBD-3 was 16 μg/ml against *E. coli* and the effective concentration of hBDs ranged from 5 to 60 μg/ml (5–7, 13, 14). The antimicrobial potency of mBD-12 was significantly reduced at high concentrations of NaCl like hBD1, hBD-2, hBD-4, mBD-1, and mBD-6 (Student's t test, $p < 0.01$) (Fig. 4*B*) (5, 7, 13, 14).

Tissue distribution of hBD-5, hBD-6, mBD-11, mBD-12, and mEP2e

RT-PCR revealed that hBD-5 and hBD-6 were specifically expressed in the human epididymis (Fig. 5*A*). No signal was detected in the other main organs: brain, trachea, lung, heart, liver, kidney, skeletal muscle, and testis. This expression pattern was similar to that of hBD-4. Although a previous report has shown the main expression of hBD-4 in the testis, our data more precisely indicate the hBD-4 expression in the human epididymis but not in the testis (7). HE2β1 expression has never been evaluated well. Our RT-PCR amplification of human epididymis RNA revealed a 546-bp fragment consistent with HE2α1 and a 470-bp fragment consistent with HE2β1, confirmed by sequencing. Although weak signals were also detected in the trachea or lung, the specific amplification of HE2 family was not confirmed by sequencing in this tissue, indicating that HE2 expression would be also confined to the epididymis.

To evaluate the mBD-11, mBD-12, and mEP2e expression, we isolated total RNA from the intestine, stomach, liver, kidney, heart, brain, esophagus, tongue, lung, trachea, skeletal muscle, epididymis, and testis of a male ICR mouse aged 4 mo. RT-PCR of mBD-11, mBD-12, and mEP2e also revealed the epididymis-specific tissue distribution (Fig. 5*B*). The tissue specificity of these isoforms was clearly different from mBD-3. RT-PCR revealed mBD-3 expression in the mouse esophagus and tongue, consistent with previous reports (18–20). Interestingly, we also detected weak mBD-3 expression in the mouse epididymis, which had not been evaluated well (18). The mBD-3 expression in the epididymis was demonstrated more clearly in Fig. 6 using the 35-cycle PCR. RT-PCR analysis of mBD-1, mBD-2, and mBD-6 also showed their expression in the mouse epididymis, whereas mBD-4 expression was not detected (data not shown).

PCR amplification of mBD-12 revealed one larger 700-bp fragment and one shorter 385-bp fragment using the specific primers from the exon 1 and the 3′ noncoding region. Sequencing of the PCR products indicated the larger one corresponding to mBD-12

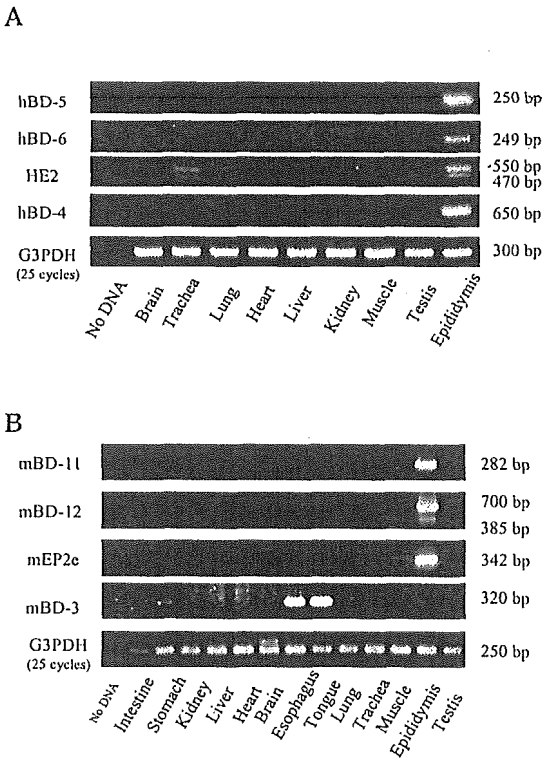

FIGURE 5. Tissue distribution of novel β-defensin isoforms in humans (*A*) and mice (*B*). RT-PCR of the indicated β-defensin isoforms and G3PDH was performed from the total RNA of the indicated tissues in humans or mice. PCR of β-defensin cDNA was conducted for 30 cycles and PCR of G3PDH was conducted for 25 cycles. hBD-4, hBD-5, hBD-6, HE2β1, and their mouse homologs are all predominantly expressed in the epididymis. The amplification of HE2 cDNA revealed a 546-bp fragment, consistent with HE2α1, and a 470-bp fragment, consistent with HE2β1. The amplification of mBD-12 also revealed a weak 385-bp fragment corresponding to the alternative spliced product. mBD-3 expression was detected in the esophagus, tongue, stomach, and epididymis.

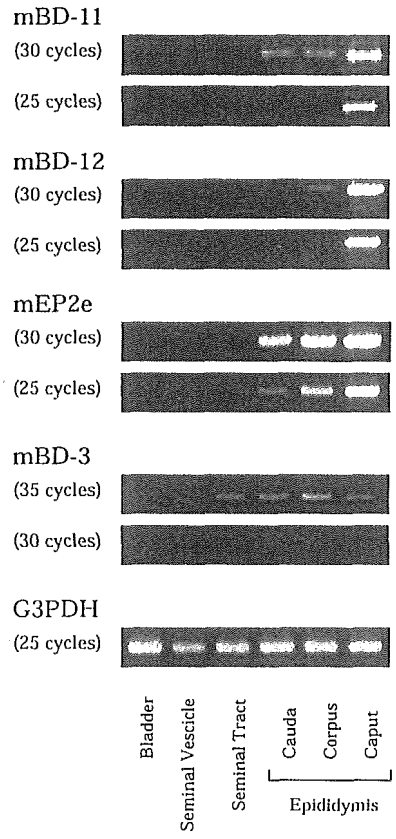

FIGURE 6. RT-PCR analysis of the regional specificity of the mBD family in the epididymis. We isolated total RNA from the mouse bladder, seminal vesicle, seminal duct, and the epididymis caput, corpus, and caudal region separately. RT-PCR detected mBD-11 and mBD-12 expression most prominent in the epididymis caput region especially after 25 cycles, and completely absent in the seminal tract, seminal vesicle, and bladder. mEP2e expression was also most prominent in the caput region, but the compatible expression was also detected in the corpus region even after 25 cycles. RT-PCR of mBD-3 showed ubiquitous expression in the caput region, corpus region, and caudal region. mBD-3 expression was detected even in the seminal tract.

and the shorter one corresponding to the novel transcripts that contained the identical sequences with the 5′ end of mBD-12 exon 1 and the 3′ noncoding region of mBD-12 exon 3, suggesting that they were alternatively spliced exons encoded by a single gene.

Region specificity of mBD-11, mBD-12, and mEP2e expression in the mouse epididymis

Our evaluation of tissue distribution suggested the importance of the β-defensin family in the male reproductive organ. To further investigate the precise distribution of their expression, we isolated total RNA from the caput, corpus, and caudal region of the adult mouse epididymis separately. We also isolated total RNA from the mouse seminal duct, seminal vesicle, and bladder. RT-PCR revealed that mBD-11 and mBD-12 expression was most prominent in the epididymis caput region and was completely absent in the seminal tract, seminal vesicle, and bladder (Fig. 6). mEP2e expression was also most prominent in the caput region, but the compatible expression was also detected in the corpus region. RT-PCR of mBD-3 showed ubiquitous expression in the caput, corpus, and caudal region and even in the seminal tract. mBD-1, mBD-2,

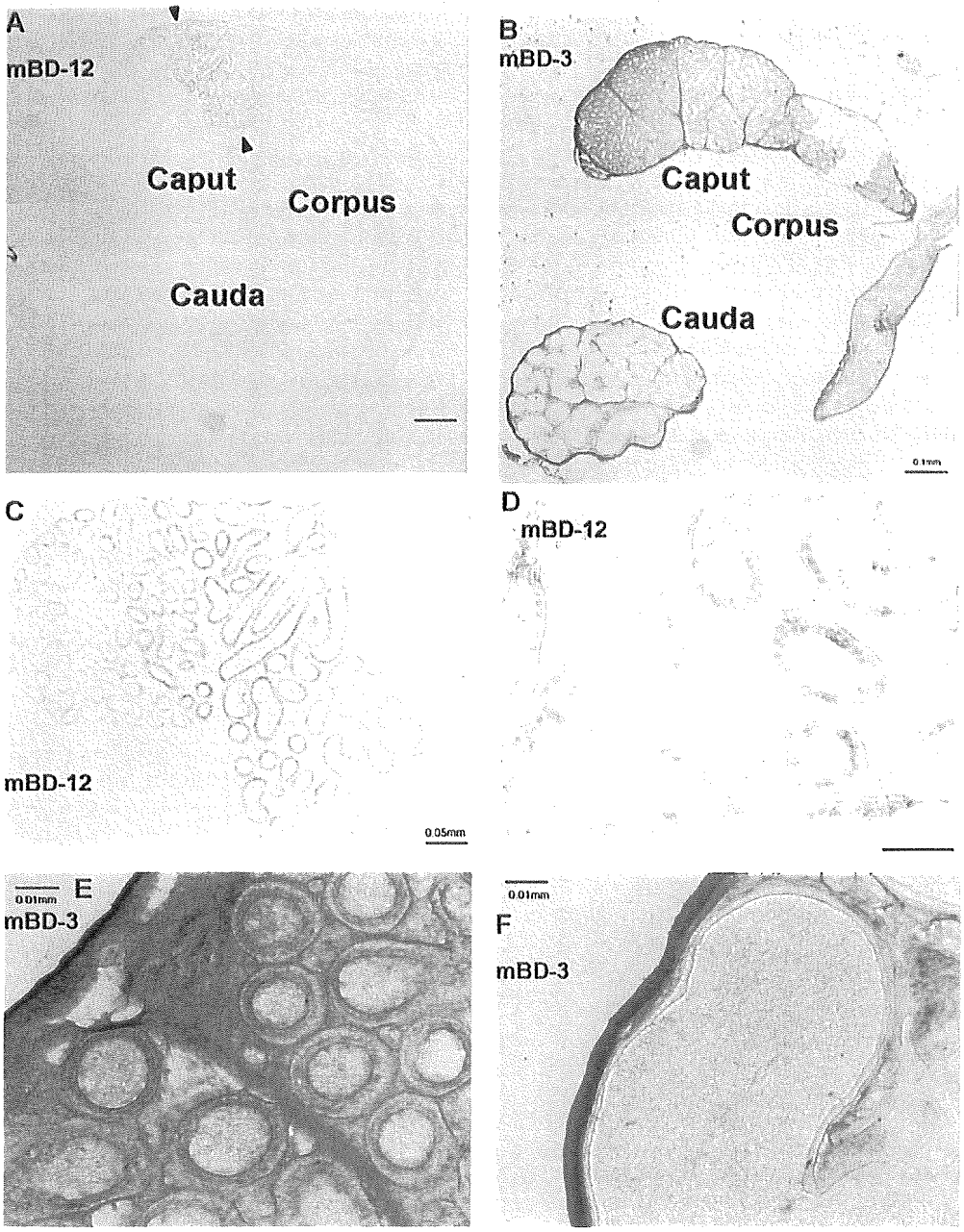

FIGURE 7. In situ hybridization of the epididymis with mBD-12 and mBD-3 antisense probe. The cryosectioned epididymis slides were hybridized with the indicated antisense probe. *A*, Low magnification. The hybridization signals of the mBD-12 antisense probe were confined to the epithelial cells of the epididymis caput mid/distal segment indicated by the arrows. No signals were detected in the corpus or caudal region. *B*, Low magnification. The hybridization signals of the mBD-3 antisense probe were present in the capsule and septum of the whole epididymis. *C*, The higher magnification of the caput region revealed more clearly the confined distribution of mBD-12 mRNA. *D*, The higher magnification of the box in Fig. 8*B* indicated the mBD-12 regulation at the cellular level. Some epithelial cells exhibited strong signals, whereas adjacent epithelial cells exhibited none, indicating the cell specificity of its expression. *E* and *F*, The higher magnification of the caput region (*E*) and caudal region (*F*) also revealed more clearly mBD-3 expression in the mesenchymal cells surrounding and compartmentalizing the epididymis. The lower signals were also present in the connective tissues around the epithelial cells. Scale bars = 100 (*A* and *B*), 50 (*C*), 25 (*D*), and 10 (*E* and *F*) μm.

and mBD-6 also showed the ubiquitous expression in the whole epididymis (data not shown).

To confirm the region-specific expression of mBD-11, mBD-12, and mEP2e in the mouse epididymis, we analyzed the distribution of mBD-11, mBD-12, mEP2e, and mBD-3 mRNA at the cellular level using in situ hybridization. The hybridization signals of the mBD-11, mBD-12, or mEP2e antisense probe were confined to the epithelial cells of the mid/distal segment of the caput region, indicating the region specificity of their expression (Figs. 7 and 8). Higher magnification also revealed more complex regulation of mBD-12 or mEP2e expression; i.e., some epithelial cells exhibited strong signals whereas the adjacent epithelial cells exhibited none in the same segment, indicating the cell specificity of their expression (Fig. 7*D*). The sense probes gave no hybridization signals (data not shown).

Parallel sections were hybridized to mBD-3 probes that gave distinct expression patterns. The most strong mBD-3 hybridization signals were present in the mesenchymal cells surrounding and compartmentalizing the epididymis, while lower signals were present in the connective tissues around the epithelial cells. This expression pattern was conserved in the caput, corpus, and caudal region, consistent with our data of RT-PCR (Fig. 7).

We compared the region specificity among mBD-11, mBD-12, and mEP2e by hybridization of adjacent sections with each probe. Their signals were almost colocalized in the mid/distal segment of the caput region (Fig. 8). However, a narrow portion adjacent to the initial segment exhibited mBD-12 hybridization signals more intensely and a relatively wide distal portion exhibited mEP2e hybridization signals more intensely, consistent with the RT-PCR analysis.

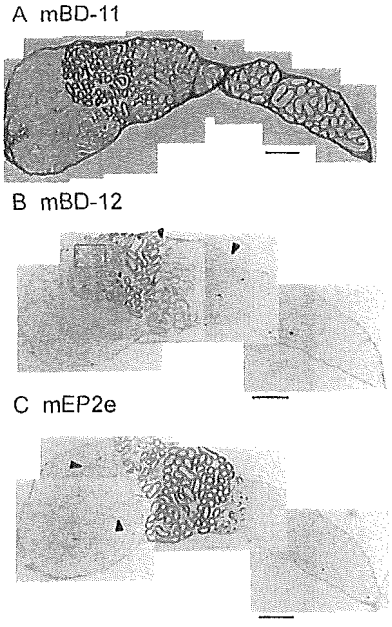

FIGURE 8. In situ hybridization of mBD-11, mBD-12, and mEP2e mRNA in the epididymis. The parallel section was hybridized with mBD-11 (*A*), mBD-12 (*B*), or mEP2e (*C*) antisense probe. Because *B* and *C* are adjacent sections, the region specificity of mBD-12 and mEP2e expression can be precisely evaluated. *A*, mBD-11 signals were confined to the mid/distal segment of the caput region. *B*, mBD-12 signals were also confined to the mid/distal segment of the caput region. The distal region shown by the arrowheads exhibited no mBD-12 signals, although mEP2e signals were intense in this region, shown in *C*. The higher magnification of the box was shown in Fig. 7*D*. *C*, mEP2e signals were also confined to the mid/distal segment of the caput region. However, the narrow region shown by the arrowheads exhibited no mEP2e signals, although mBD-12 signals were intense in this region, shown in *B*. Scale bars = 100 μm.

Discussion

In this work we describe the identification of the epididymis-specific β-defensin isoforms including two novel hBD, termed hBD-5 and hBD-6, and the mouse homologs of hBD-5, hBD-6, and HE2β1, termed mBD-12, mBD-11, and mEP2e, respectively.

The organization of gene cluster is a peculiar feature of the defensin family and prompted us to use the human genomic sequence to search novel defensin genes. Because multiple isoforms of the β-defensin family had been identified in human and mouse organs and may compensate each other for their common functions in part, the overall identification of β-defensin isoforms is very important to study their physiological roles.

hBD-5, hBD-6, hBD-4, and HE2β1 were specifically expressed in the human epididymis. Because the epididymis is anatomically continuous to the urethra, it is always at the risk of ascending microbial invasion. Acute epididymitis is a common sexually transmitted disease, caused by bacterial infection of the epididymis. Therefore, host defense against a bacterial pathogen would be very important in the epididymis for the protection of spermatozoa.

Our identification of the novel mBD, mBD-12, and mEP2e would also be noteworthy because animal models are very useful to understand the physiological and pathological significance of these peptides. The comparison of the genomic organization of HE2β1 and mEP2e revealed that HE2β1 and mEP2e would be included in different message variants. Although the genomic sequence of the HE2 gene indicated the possible existence of another promoter within the second intron of the HE2β1 gene, no transcripts corresponding to the EP2e isoform have been identified in humans. Considering that no splicing variants corresponding to the HE2β1 isoform were detected in mice, the major transcript would be different between humans and mice, at least at a basal state.

Our identification of the epididymis-specific β-defensin isoforms clarified the existence of two groups in the β-defensin family: epididymis-specific isoforms and the other isoforms. The former includes HE2β1, hBD-4, hBD-5, and hBD-6 and the latter includes hBD-1, hBD-2, and hBD-3 in humans. Interestingly, the epididymis-specific β-defensin genes were located within a region encompassing ~40 kb in the human defensin gene cluster on chromosome 8. In mice, this report first indicated that mBD-11, mBD-12, and mEP2e are expressed, and that their expression is epididymis specific. Between the two groups, some different features are present in their amino acid sequences. First, the amino acid sequences of the epididymis-specific β-defensin isoforms were well conserved between humans and mice in comparison with the other β-defensin isoforms. Although mBD-3 had been regarded as a hBD-2 homolog, the amino acid sequence identity was only 40%. In contrast, mBD-11, mBD-12, and mEP2e were >65% identical with their human homologs. Second, some amino acid residues are different between the two groups. The glutamic acid residue is conserved in six positions before the C4 residue in the epididymis-specific β-defensin isoforms, and this feature is conserved even in the α-defensin family. Although few conserved residues have been indicated, except the cysteine motif, between the α-defensin and β-defensin families and it had been questioned whether the two families have really descended from a single ancestral gene, this common feature would support the evolutionary continuity between the α-defensin and β-defensin families (36). In addition, these features would reflect the existence of some specific microenvironmental condition of host defense in the epididymis.

Our evaluation of the mBD-11, mBD-12, mEP2e, and mBD-3 expression pattern in the epididymis revealed mBD-11, mBD-12,

and mEP2e expression in the epithelial cells of the mid/distal segment of the caput region and mBD-3 expression in the capsule and septum of the whole epididymis. These findings also clarify the different features between the epididymis-specific isoforms and the other β-defensin isoforms.

More interestingly, mBD-11, mBD-12, and mEP2e were expressed in different regions, although major portions of the middle segment expressed both genes. In general, the epididymis displays a highly region-specific and cell-specific pattern of gene expression (37, 38). This spatial regulation would make different luminal environments, and in these specific environments the specific functions of the epididymis would be conducted, such as regulation of sperm maturation, storage of mature spermatozoa, and protection from pathogens or reactive oxygen. Our results indicate that some different regional regulation would be also working among the members of the epididymis-specific β-defensin family, suggestive of their roles in the specific functions of the epididymis, although this issue remains to be investigated more clearly.

Acknowledgments

We thank Drs. H. Hojo (Tokai University, Hiratsuka, Japan), T. Takeuchi (University of Tokyo), K. Yamaguchi, and A. Kato (Mitsui Memorial Hospital) for valuable suggestions and helpful assistance.

References

1. Ganz, T., M. E. Selsted, D. Szklarek, S. S. L. Harwig, K. Daher, D. F. Bainton, and R. I. Lehrer. 1985. Defensins: natural peptide antibiotics of human neutrophils. *J. Clin. Invest. 76:1427.*
2. Diamond, G., M. Zasloff, H. Eck, M. Brasseur, W. L. Maloy, and C. L. Bevins. 1991. Tracheal antimicrobial peptide, a cysteine-rich peptide from mammalian tracheal mucosa: peptide isolation and cloning of a cDNA. *Proc. Natl. Acad. Sci. USA 88:3952.*
3. Schonwetter, B. S., E. D. Stolzenberg, and M. A. Zasloff. 1995. Epithelial antibiotics induced at sites of inflammation. *Science 267:1645.*
4. Bensch, K. W., M. Raida, H. J. Magert, P. Schulz-Knappe, and W. G. Forssmann. 1995. hBD-1: a novel β-defensin from human plasma. *FEBS Lett. 368:331.*
5. Harder, J., J. Bartels, E. Christophers, and J. M. Schröder. 1997. A peptide antibiotic from human skin. *Nature 387:861.*
6. Harder, J., J. Bartels, E. Christophers, and J. M. Schröder. 2001. Isolation and characterization of human β-defensin-3, a novel human inducible peptide antibiotic. *J. Biol. Chem. 276:5707.*
7. Garcia, J. R., A. Krause, S. Schulz, F. J. Rodriguez-Jimenez, E. Kluver, K. Adermann, U. Forssmann, A. Frimpong-Boateng, R. Bals, and W. G. Forssmann. 2001. Human β-defensin 4: a novel inducible peptide with a specific salt-sensitive spectrum of antimicrobial activity. *FASEB J. 15:1819.*
8. Osterhoff, C., C. Kirchhoff, N. Krull, and R. Ivell. 1994. Molecular cloning and characterization of a novel human sperm antigen (HE2) specifically expressed in the proximal epididymis. *Biol. Reprod. 50:516.*
9. Hamil, K. G., P. Sivashanmugam, R. T. Richardson, G. Grossman, S. M. Ruben, J. L. Mohler, P. Petrusz, M. G. O'Rand, F. S. French, and S. H. Hall. 2000. HE2β and HE2γ, new members of an epididymis-specific family of androgen-regulated proteins in the human. *Endocrinology 141:1245.*
10. Fröhlich, O., C. Po, and L. G. Young. 2001. Organization of the human gene encoding the epididymis-specific EP2 protein variants and its relationship to defensin genes. *Biol. Reprod. 64:1072.*
11. Jia, H. P., B. C. Schutte, A. Schudy, R. Linzmeier, J. M. Guthmiller, G. K. Johnson, B. F. Tack, J. P. Mitros, A. Rosenthal, T. Ganz, and P. B. McCray, Jr. 2001. Discovery of new human β-defensins using a genomics-based approach. *Gene 263:211.*
12. Goldman, M. J., M. G. Anderson, E. D. Stolzenberg, P. U. Kari, M. Zasloff, and J. M. Wilson. 1997. Human β-defensin-1 is a salt-sensitive antibiotic in lung that is inactivated in cystic fibrosis. *Cell 88:553.*
13. Valore, E. V., C. H. Park, A. J. Quayle, K. R. Wiles, P. B. McCray, Jr., and T. Ganz. 1998. Human β-defensin-1: an antimicrobial peptide of urogenital tissues. *J. Clin. Invest. 101:1633.*
14. Bals, R., X. Wang, Z. Wu, T. Freeman, V. Bafna, M. Zasloff, and J. M. Wilson. 1998. Human β-defensin 2 is a salt-sensitive peptide antibiotic expressed in human lung. *J. Clin. Invest. 102:874.*
15. Huttner, K. M., C. A. Kozak, and C. L. Bevins. 1997. The mouse genome encodes a single homolog of the antimicrobial peptide human β-defensin 1. *FEBS Lett. 413:45.*
16. Bals, R., M. J. Godman, and J. M. Wilson. 1998. Mouse β-defensin 1 is a salt-sensitive antimicrobial peptide in epithelia of the lung and urogenital tract. *Infect. Immun. 66:1225.*
17. Morrison, G. M., D. J. Davidson, and J. R. Dorin. 1999. A novel mouse β defensin, Defb2, which is upregulated in the airways by lipopolysaccharide. *FEBS Lett. 442:112.*
18. Bals, R., X. Wang, R. L. Meegalla, S. Wattler, D. Weiner, M. C. Nehls, and J. M. Wilson. 1999. Mouse β-defensin 3 is an inducible antimicrobial peptide expressed in the epithelia of multiple organs. *Infect. Immun. 67:3542.*
19. Jia, H. P., S. A. Wowk, B. C. Schutte, S. K. Lee, A. Vivado, B. F. Tack, C. L. Bevins, and P. B. McCray, Jr. 2000. A novel murine β-defensin expressed in tongue, esophagus, and trachea. *J. Biol. Chem. 275:33314.*
20. Yamaguchi, Y., S. Fukuhara, T. Nagase, T. Tomita, S. Hitomi, S. Kimura, H. Kurihara, and Y. Ouchi. 2001. A novel mouse β-defensin, mBD-6, predominantly expressed in skeletal muscle. *J. Biol. Chem. 276:315.*
21. Bauer, F., K. Schweimer, E. Kluver, J. R. Conejo-Garcia, W. G. Forssmann, P. Rosch, K. Adermann, and H. Sticht. 2001. Structure determination of human and murine β-defensins reveals structural conservation in the absence of significant sequence similarity. *Protein Sci. 10:2470.*
22. Zhao, C., I. Wang, and R. I. Lehrer. 1996. Widespread expression of β-defensin hBD-1 in human secretory glands and epithelial cells. *FEBS Lett. 396:319.*
23. Fulton, C., G. M. Anderson, M. Zasloff, R. Bull, and A. G. Quinn. 1997. Expression of natural peptide antibiotics in human skin. *Lancet 350:1750.*
24. McCray, P. B., Jr., and L. Bentley. 1997. Human airway epithelia express a β-defensin. *Am. J. Respir. Cell Mol. Biol. 16:343.*
25. O'Neil, D. A., E. M. Porter, D. Elewaut, G. M. Anderson, L. Eckmann, T. Ganz, and M. F. Kagnoff. 1999. Expression and regulation of the human β-defensins hBD-1 and hBD-2 in intestinal epithelium. *J. Immunol. 163:6718.*
26. Garcia, J. R., F. Jaumann, S. Shulz, A. Krause, J. Rodriguez-Jimenez, U. Forssmann, K. Adermann, E. Kluver, C. Vogelmeier, D. Becker, et al. 2001. Identification of a novel, multifunctional β-defensin (human β-defensin 3) with specific antimicrobial activity: its interaction with plasma membranes of *Xenopus* oocytes and the induction of macrophage chemoattraction. *Cell Tissue Res. 306: 257.*
27. Li, P., H. C. Chan, B. He, S. C. So, Y. W. Chung, Q. Shan, Y. D. Zhang, and Y. L. Zhang. 2001. An antimicrobial peptide gene found in the male reproductive system of rats. *Science 291:1783.*
28. Fröhlich, O., C. Po, T. Murphy, and L. G. Young. 2000. Multiple promoter and splicing mRNA variants of the epididymis-specific gene EP2. *J. Androl. 21:421.*
29. Liu, L., L. Wang, H. P. Jia, C. Zhao, H. H. Q. Heng, B. C. Schutte, P. B. McCray, Jr., and T. Ganz. 1998. Structure and mapping of the human β-defensin HBD-2 gene and its expression at sites of inflammation. *Gene 222:237.*
30. Linzmeier, R., C. H. Ho, B. V. Hoang, and T. Ganz. 1999. A 450-kb contig of defensin genes on human chromosome 8p23. *Gene 233:205.*
31. Schutte, B. C., J. P. Mitros, J. A. Bartlett, J. D. Walters, H. P. Jia, M. J. Welsh, T. L. Casavant, and P. B. McCray, Jr. 2002. Discovery of five conserved β-defensin gene clusters using a computational search strategy. *Proc. Natl. Acad. Sci. USA 99:2129.*
32. Kawai, J., A. Shinagawa, K. Shibata, M. Yoshino, M. Itoh, Y. Ishii, T. Arakawa, A. Hara, Y. Fukunishi, H. Konno, et al. 2001. Functional annotation of a full-length mouse cDNA collection. *Nature 409:685.*
33. Harwig, S. S., T. Ganz, and R. I. Lehrer. 1994. Neutrophil defensins: purification, characterization, and antimicrobial testing. *Methods Enzymol. 236:160.*
34. Becker, M. N., G. Diamond, M. W. Verghese, and S. H. Randell. 2000. CD14-dependent lipopolysaccharide-induced β-defensin-2 expression in human tracheobronchial epithelium. *J. Biol. Chem. 275:29731.*
35. Lehrer, R. I., and T. Ganz. 1990. Antimicrobial polypeptides of human neutrophils. *Blood 76:2169.*
36. Hughes, A. L. 1999. Evolutionary diversification of the mammalian defensins. *Cell. Mol. Life Sci. 56:94.*
37. Rodriguez, C. M., J. L. Kirby, and B. T. Hinton. 2000. Regulation of gene transcription in the epididymis. *Reproduction 122:41.*
38. Orgebin-Crist, M. C. 1995. Androgens and epididymal function. In *Pharmacology, Biology, and Clinical Applications of Androgens.* D. Bhasin, H. L. Gabelnick, J. M. Spieler, R. S. Swerdloff, and C. Wang, eds. Wiley-Liss, New York, p. 27.

Respirology (2002) **7**, 305–310

ORIGINAL ARTICLE

Molecular mechanisms underlying human β-defensin-2 gene expression in a human airway cell line (LC2/ad)

TETSUJI TOMITA, TAKAHIDE NAGASE, EIJIRO OHGA, YASUHIRO YAMAGUCHI, MASAO YOSHIZUMI AND YASUYOSHI OUCHI

Department of Geriatric Medicine, Graduate School of Medicine, University of Tokyo, Tokyo, Japan

Molecular mechanisms underlying human β-defensin-2 gene expression in a human airway cell line (LC2/ad)
TOMITA T, NAGASE T, OHGA E, YAMAGUCHI Y, YOSHIZUMI M, OUCHI Y. *Respirology* 2002; **7**: 305–310

Objective: Recently, human β-defensin-2 (hBD-2), an inducible defensin, has been reported to be involved in innate immunity and host defence. To examine the exact roles of hBD-2 in the respiratory system, we examined the molecular mechanisms of hBD-2 gene expression *in vitro*.

Methodology: Using a human airway cell line (LC-2/ad), lipopolysaccharide (LPS)-induced gene expression of hBD-2 was studied in the absence or the presence of (i) dexamethasone, (ii) inhibition of NF-κB and AP-1, (iii) intracellular calcium chelator, and (iv) cyclooxygenase (COX) inhibitors.

Results: Lipopolysaccharide-induced gene expression of hBD-2 was down-regulated by (i) dexamethasone, (ii) inhibition of NF-κB and AP-1, and (iii) intracellular calcium chelator. However, COX inhibitors had no effect on LPS-induced mRNA expression of hBD-2.

Conclusion: These findings suggest that glucocorticoids (GC), but not COX inhibitors, reduce hBD-2 gene expression, while NF-κB, AP-1 and intracellular calcium are essential for hBD-2 expression. Glucocorticoid-induced down-regulation of hBD-2 might be involved in the GC-induced suppression of respiratory host defence associated with hBD-2.

Key words: cyclooxygenase inhibitors, glucocorticoids, human β-defensin-2, intracellular calcium, NF-κB.

INTRODUCTION

Antimicrobial peptides including β-defensins are thought to be effective against opportunistic infections.[1,2] In humans, three β-defensins have been identified. The first human β-defensin, hBD-1, is predominantly expressed in epithelia of the urogenital tract and has been reported to be constitutive.[3–5] The second and third human β-defensins, hBD-2 and hBD-3, were isolated from psoriatic skin and found to be predominantly expressed in the skin and respiratory tract.[6,7] Of note, hBD-2 gene expression is inducible by various proinflammatory agents such as TNF-α, IL-1β, IL-8, lipopolysaccharide (LPS), bacteria, and yeasts.[6,8–11] It has been shown that LPS-induced expression of hBD-2 in human tracheobronchial epithelial cells requires CD14, which may complex with a Toll-like receptor (TLR) to ultimately activate NF-κB.[9] In addition, β-defensins have been recently reported to promote immune responses by recruiting dendritic and T cells through interaction with CCR6.[12]

Recently, it has been suggested that hBD-2 could be involved in the respiratory immune system.[10] Human airway epithelial cells express hBD-2, which is induced by inflammation and bacteria including *Pseudomonas aeruginosa*. It has also been demonstrated that hBD-2 has a broad spectrum of antimicrobial activity against both bacteria[6,13] and fungi,[6] which are common pathogens provoking respiratory infection. Therefore, it is postulated that hBD-2 is an epithelium-derived antimicrobial peptide that contributes to respiratory host defence.[10]

In the current study, we examined the molecular mechanisms of hBD-2 expression *in vitro*. To perform the present study, we used a human airway cell line, LC-2/ad, which was established from pleural effu-

Correspondence: Dr T. Tomita, Department of Geriatric Medicine, Graduate School of Medicine, University of Tokyo, Hongo 7-3-1, Bunkyo-ku, Tokyo 113-8655, Japan. Email: tomita-tky@umin.ac.jp

Received 2 January 2002; revised 5 June 2002; accepted for publication 25 June 2002.

sion of pulmonary adenocarcinoma and exhibits an epithelial appearance.[14]

MATERIALS AND METHODS

All materials were obtained from Sigma Chemical Co. (St. Louis, MO, USA) unless otherwise noted.

Cell culture

LC2/ad were obtained from RIKEN (Ibaraki, Japan) and grown in RPMI 1640 (Nissui, Tokyo, Japan)/ Ham F12 (Nissui) medium containing 15% fetal bovine serum (FBS).[14] LC2/ad from passage 3–10 were grown to confluency in 78.54 cm^2 culture dishes (100 mm in diameter). The entire apparatus was placed in a CO_2 incubator at 37°C in 5% CO_2/95% humidified air.

The effect of lipopolysaccharide on human β-defensin-2 gene expression

LC2/ad were stimulated with *Pseudomonas aeruginosa*-derived LPS, serotype 10. A time course of hBD-2 mRNA induction by LPS (1 μg/mL) was performed from 0 to 48 h. Dose-dependent responses induction of hBD-2 mRNA by LPS was examined at 24 h. We aspirated medium from culture dishes after stimulation with LPS and washed the cells twice. RNA was extracted frin each sample and analysed by Northern blot.

Regulation of human β-defensin-2 by transcriptional factors and intracellular calcium chelator

To study the role of NF-κB in LPS-induced hBD-2 gene expression, pyrrolidine dithiocarbamate (PDTC), an NF-κB inhibitor, was added to the medium. The concentration of FBS in the medium was 5% during the experiments. LC2/ad were pretreated with PDTC for 2 h and subsequently stimulated with LPS for 12 h.

The role of AP-1 in the LPS-induced hBD-2 gene expression was examined by adding 12-*O*-tetradecanoylphorbol-13-acetate (TPA) to the medium. LC2/ad were stimulated with TPA (10^{-7} M) for indicated times. In addition, LC2/ad were pretreated with TPA (10^{-7} M) for 24 h and subsequently stimulated with LPS (1 μg/mL) for 1–24 h.

In order to elucidate the role of intracellular calcium in LPS-induced elevation of hBD-2 gene expression, bis-(o-aminophenoxy)-ethane-N,N, N′,N′–tetraacetic acid, tetra (acetoxymethyl)-ester (BAPTA-AM, intracellular calcium chelator) (Dojin Chemical Institute, Kumamato, Japan) was added to the medium. LC2/ad were pretreated with BAPTA-AM for 2 h and subsequently stimulated with LPS (1 μg/mL) for 24 h.

Regulation of human β-defensin-2 by glucocorticoids

In order to study the effects of glucocorticoids, a range of dexamethasone concentrations were added to the medium. LC2/ad were pretreated with dexamethasone for 2 h and subsequently stimulated with LPS (1 μg/mL) for 24 h. RNA was extracted frin each sample and analysed by Northern blot.

Regulation of human β-defensin-2 by cyclooxygenase inhibitors

In order to study the effects of COX inhibitors, indomethacin, aspirin or NS-398 (Cayman Chemical, MI, USA) were added to the medium. LC2/ad were pretreated with each COX inhibitor for 2 h and subsequently stimulated with LPS (1 μg/mL) for 24 h.

Reverse transcription polymerase chain reaction amplification

The reverse transcription polymerase chain reaction (RT-PCR) hBD-2 cDNA product was obtained by using oligonucleotides, 5′-CCAGCCATCAGCCATGAG GGT-3′ as an antisense primer, 5′-GGAGCCCTTTCT GAATCGCA-3′ as a sense primer, and RNA from LC2/ ad cells as a template. The RT-PCR was performed using a Titan one tube RT-PCR kit. The general protocol for RT-PCR amplification was modified as follows: initial denaturation was 1 min at 95°C; 40 cycles of amplification was performed by cycling 1.15 min at 94°C, 30 s at 60°C, and 1 min at 68°C. Bands were purified by electroelution after electrophoresis in polyacrylamide gels.

Human β-defensin-2 cDNA probe and Northern blot analysis

The above-mentioned RT-PCR amplification was used to generate an hBD-2 cDNA fragment. The human β-defensin-2 cDNA fragment was ligated into pCR 2.1 vector (Invitrogen, Carlsbad, CA, USA). We aspirated medium from culture dishes stimulated with various drugs and then washed the cells twice. Total cellular RNA was extracted by the acid guanidinium thyocynate-phenol-chloroform method[15] from LC2/ad and quantitated by measuring absorbance at 260 nm. RNA samples (25 μg) were electrophoresed through 1.2% formaldehyde/agarose gels and transferred to nylon membranes (Biodyne Plus Membrane, PALL Corporation, Hills, NY, USA) by standard procedures.[16] The membranes were hybridized with a random primed, ^{32}P-labelled, Eco RI fragment of hBD-2 cDNA. The hybridization was performed for 2 h using Quick Hybridization Solution (Stratagene, La Jolla, CA, USA). The hybridized membranes were then washed and autoradiographed. The membranes were subsequently re-hybridized with a ^{32}P-labelled 18S oligonucleotide

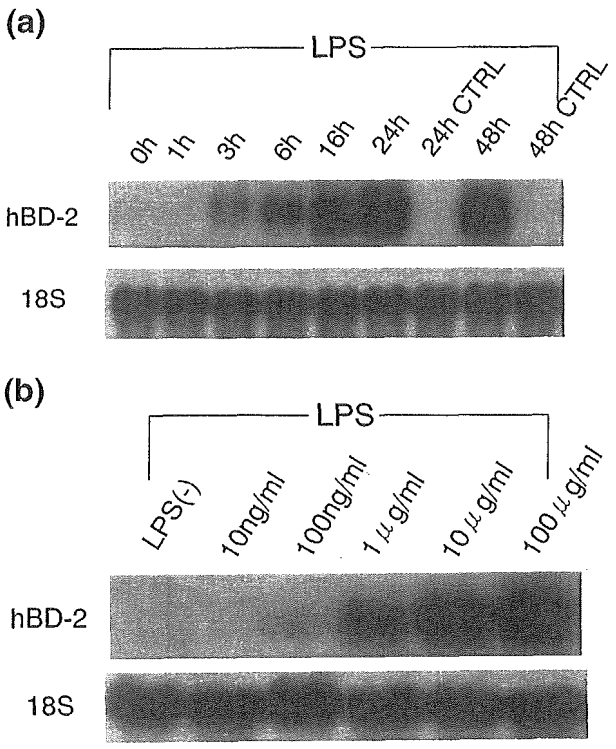

Figure 1 (a) Time course of human β-defensin-2 (hBD-2) mRNA induction by lipopolysaccharide (LPS). The human airway cell line LC2/ad was stimulated by LPS (10 μg/mL), and total RNA was extracted at the indicated times. Northern blot analysis was performed with 25 μg of total RNA hybridized with hBD-2 cDNA probe. The membrane was rehybridized with 18S probe. (b) Dose responses of hBD-2 mRNA induction by LPS. LC2/ad were stimulated with LPS, and total RNA was extracted after 24 h. Northern blot analysis was performed with 25 μg of total RNA hybridized with hBD-2 cDNA probe. The membrane was rehybridized with 18S probe.

(ACGGTATCTGATCGTCTTCGAACC) as an internal standard for total RNA content.

RESULTS

The baseline level of hBD-2 mRNA was not detectable, while LPS increased hBD-2 mRNA levels in LC2/ad in both a time- (Fig. 1a) and dose-dependent manner (Fig. 1b). Lipopolysaccharide-induced elevation of hBD-2 mRNA was inhibited by PDTC (NF-κB inhibitor).

To study the role of NF-κB in LPS-induced hBD-2 gene expression, LC2/ad were pretreated with PDTC for 2 h and subsequently stimulated with LPS for 12 h. Lipopolysaccharide-induced elevation of hBD-2 mRNA was partially inhibited by PDTC pretreatment, suggesting that LPS-induced elevation of hBD-2 gene expression is dependent on NF-κB activity in part (Fig. 2).

LC2/ad were then stimulated by TPA (10^{-7} M). While increased mRNA levels of heparin-binding epidermal

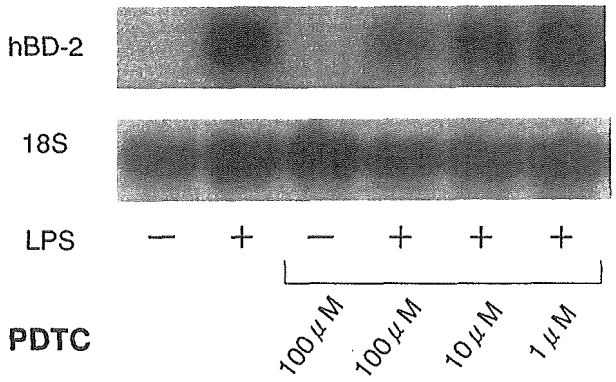

Figure 2 Lipopolysaccharide (LPS)-induced up-regulation of human β-defensin-2 (hBD-2) mRNA was inhibited by a NF-κB inhibitor, pyrrolidine dithiocarbamate (PDTC). LC2/ad cells were stimulated with LPS (1 μg/mL) in the absence or presence of PDTC for 12 h. Northern blot analysis was performed with 25 μg of total RNA hybridized with hBD-2 cDNA probe. The membrane was rehybridized with 18S probe.

growth factor like growth factor (HB-EGF) were observed following 1–4 h TPA pretreatment, hBD-2 gene expression was not detected at any time point (Fig. 3a). This result indicated that TPA stimulation was sufficient for the induction of HB-EGF, but not for that of hBD-2. LC2/ad were pretreated with TPA (10^{-7} M) for 24 h to down-regulate protein kinase C (PKC) activity. Cells were subsequently stimulated with LPS for 1–24 h. Lipopolysaccharide-induced elevation of hBD-2 mRNA was inhibited by TPA pretreatment, suggesting that LPS-induced elevation of hBD-2 gene expression is partly dependent on PKC activity (Fig. 3b).

To examine the role of intracellular calcium in LPS-induced up-regulation of hBD-2 gene, LC2/ad were stimulated with LPS in the absence or presence of BAPTA-AM, an intracellular calcium chelator. Lipopolysaccharide-induced elevation of hBD-2 mRNA levels was completely inhibited by BAPTA-AM (Fig. 4). This finding suggests that intracellular calcium is necessary for LPS-induced hBD-2 gene expression.

Subsequently, LC2/ad were stimulated with LPS in the absence or presence of dexamethasone (glucocorticoid), indomethacin, aspirin (COX inhibitor), and NS-398 (COX-2 selective inhibitors). As shown in Fig. 5, LPS-induced elevation of hBD-2 mRNA levels was inhibited by dexamethasone. In contrast, LPS-induced hBD-2 gene expression was not affected by indomethacin, aspirin, or NS-398 (Figs 6,7).

DISCUSSION

The current data indicate that dexamethasone down-regulates LPS-induced hBD-2 gene expression in airway epithelial cells. The NF-κB pathway appears to play a key role in the expression of hBD-2, while intracellular calcium and, in part, PKC activity are also essential for LPS-induced expression of hBD-2.

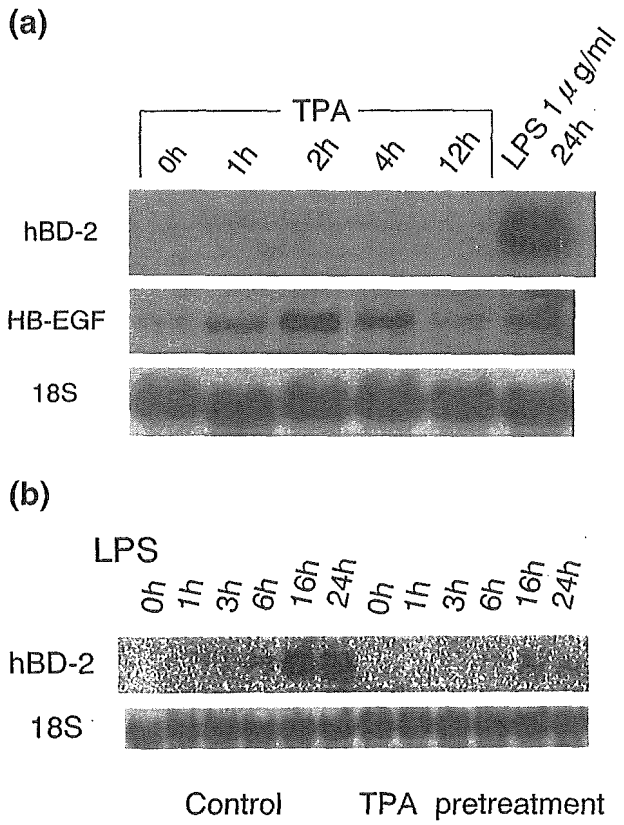

Figure 3 (a) TPA induced the expression of HB-EGF mRNA, but not that of human β-defensin-2 (hBD-2). LC2/ad were stimulated by 12-*O*-tetra-decanoylphorbol-13-acetate (TPA; 10^{-7} M) for the indicated times, or with lipopolysaccharide (LPS) for 24 h. Northern blot analysis was performed with 25 μg of total RNA hybridized with hBD-2 cDNA probe. The membrane was rehybridized with HB-EGF probe and 18S probe. (b) LPS-induced up-regulation of hBD-2 mRNA was partially inhibited by TPA pretreatment. LC2/ad were pretreated with TPA (10^{-7} M) for 24 h and subsequently stimulated with LPS (1 μg/mL) for 1–24 h. Northern blot analysis was performed with 25 μg of total RNA hybridized with hBD-2 cDNA probe. The membrane was rehybridized with 18S probe.

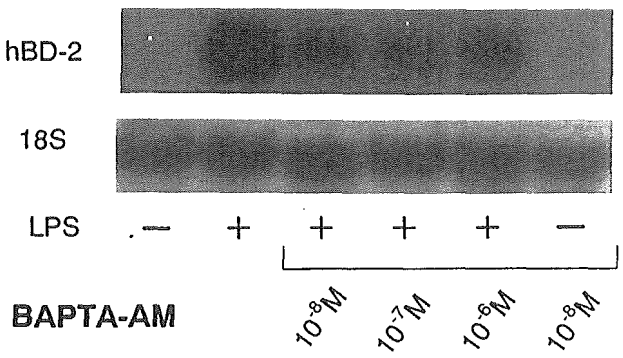

Figure 4 Lipopolysaccharide (LPS)-induced up-regulation of human β-defensin-2 (hBD-2) mRNA was inhibited by bis-(o-aminophenoxy)-ethane-N,N,N′,N′–tetraacetic acid, tetra (acetoxymethyl)-ester (BAPTA-AM). LC2/ad were stimulated with LPS (1 μg/mL) in the absence or presence of BAPTA-AM for 24 h. Northern blot analysis was performed with 25 μg of total RNA hybridized with hBD-2 cDNA probe. The membrane was rehybridized with 18S probe.

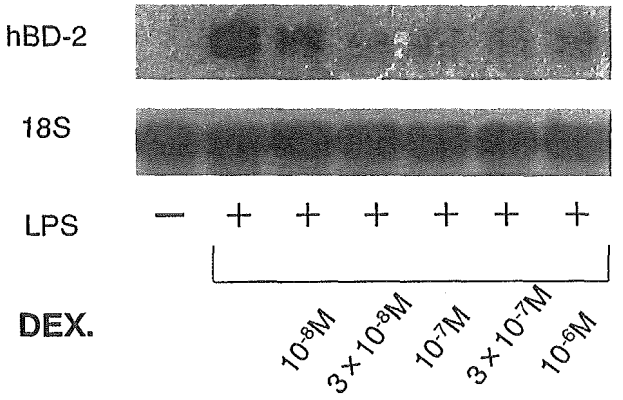

Figure 5 Lipopolysaccharide (LPS)-induced up-regulation of human β-defensin-2 (hBD-2) mRNA was inhibited by dexamethasone. LC2/ad were stimulated with LPS (1 μg/mL) in the absence or presence of dexamethasone for 24 h. Northern blot analysis was performed with 25 μg of total RNA hybridized with hBD-2 cDNA probe. The membrane was rehybridized with 18S probe. DEX, dexamethasone.

In contrast, COX inhibitors had no effect on LPS-induced hBD-2 gene expression.

β-defensins are antimicrobial peptides that control the defence of mammalian epithelial mucosa. Tracheal antimicrobial peptide (TAP) and lingual antimicrobial peptide (LAP) were the first members of the β-defensin family of mammalian antimicrobial peptides to be described.[17,18] Tracheal antimicrobial peptide is produced by bovine respiratory tract mucosa, while LAP is produced by tongue mucosa. The genes for these peptides are inducibly expressed by various proinflammatory agents such as TNF-α, IL-1β, bacteria or bacterial LPS.[19–21] In humans, three β-defensins have been identified. The first human β-defensin, hBD-1, was isolated as a trace peptide from human haemofiltrates, where its mRNA is found to be predominantly expressed in epithelia of the urogenital tract.[3–5] The second human β-defensin, hBD-2, is isolated from psoriatic skin, where its mRNA is found to be predominantly expressed in epithelia of the trachea and lung.[6,8] The third β-defensin, hBD-3, was also isolated from psoriatic skin.[7] In terms of patterns of gene expression, there is a marked difference among these β-defensins. The expression of hBD-1 has been reported to be constitutive.[4] In contrast, hBD-2 gene expression is inducible by various proinflammatory agents such as TNF-α, IL-1β, IL-8, LPS, bacteria, and yeasts.[6,8–11] The expression pattern of hBD-3 has also been reported to be inducible.[7] Therefore, hBD-2 and hBD-3 are considered to represent the human equivalent of bovine TAP and LAP. It has been suggested that these inducible β-defensins

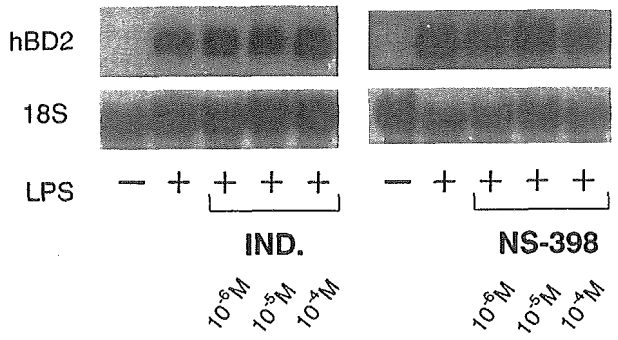

Figure 6 Lipopolysaccharide (LPS)-induced up-regulation of human β-defensin-2 (hBD-2) mRNA was not inhibited by indomethacin or NS-398. LC2/ad were stimulated with LPS (1 μg/mL) in the absence or presence of indomethacin or NS-398 for 24 h. Northern blot analysis was performed with 25 μg of total RNA hybridized with hBD-2 cDNA probe. The membrane was rehybridized with 18S probe. IND, indomethacin.

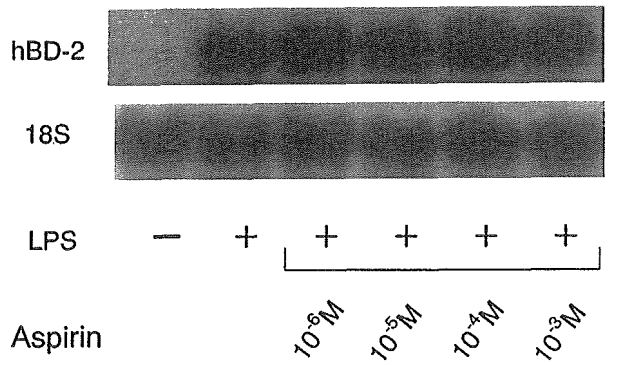

Figure 7 Lipopolysaccharide (LPS)-induced up-regulation of human β-defensin-2 (hBD-2) mRNA was not inhibited by aspirin. LC2/ad were stimulated with LPS (1 μg/mL) in the absence or presence of aspirin for 24 h. Northern blot analysis was performed with 25 μg of total RNA hybridized with hBD-2 cDNA probe. The membrane was rehybridized with 18S probe.

may play important roles in innate immunity and dynamic host defence.

Recently, the 5′-flanking region of hBD-2 has been demonstrated to contain consensus binding sequences for AP-1-like and NF-κB-like sites, suggesting that hBD-2 is inducible by acute inflammatory stimuli. Consequently, it has been assumed that AP-1 and NF-κB participate in transcriptional regulation. In support of this, it was reported that NF-κB participates in the transcriptional regulation of TAP gene expression following LPS stimulation.[21] Furthermore, it has been recently reported that LPS-induced expression of hBD-2 in human tracheobronchial epithelial cells requires CD14 and Toll-like receptors (TLR) to activate NF-κB.[9] It is presumed that: (i) mammalian TLR and associated signalling factors may represent a conserved evolutionary response to infectious pathogens, and (ii) LPS- and IL-1-inducible hBD-2 may be a conserved defence mechanism similar to the antimicrobial peptides found in Drosophila.[22] However, little is yet known about roles of AP-1 in hBD-2 expression. From the present study it is suggested that transcriptional activity of hBD-2 is related to NF-κB and, partly, AP-1. This finding is compatible with the existence of both consensus sequences in the putative promoter region. In addition, intracellular calcium is also involved in hBD-2 gene expression induced by LPS.

Glucocorticoids have been used as immunosuppressive drugs to manage inflammatory diseases. It is postulated that the activities of GC are mediated by (i) various transcription factors including NF-κB and AP-1 and (ii) T-cell-mediated immunity. While GC are useful immunosuppressive agents, high doses of GC are associated with a high incidence of infection. Currently, little is known about GC-induced susceptibility to opportunistic infection. In the present study, we obtained direct evidence that LPS-induced hBD-2 gene expression was inhibited by dexamethasone in airway epithelial cells *in vitro*.

It is possible that GC-induced down-regulation of hBD-2 is related to the increased risk of opportunistic respiratory infection in GC-treated patients. Glucocorticoids inhibit both NF-κB and AP-1 transcription factors, resulting in inhibition of hBD-2 gene expression. Since hBD-2 has both bactericidal and fungicidal activities,[6,14] GC-induced inhibition of hBD-2 might contribute to opportunistic respiratory infection. In addition, previous reports have shown that β-defensins including hBD-2 are chemotactic for immature dendritic cells and memory T cells through CCR6.[12] Therefore, GC-induced inhibition of hBD-2 is potentially involved in suppression of T-cell-mediated host defence.

In the present study, COX inhibitors including a COX-2 selective inhibitor had no effect on LPS-induced hBD-2 gene expression in cultured airway epithelial cells. It remains controversial whether host defence against infectious agents would be affected by non-steroidal anti-inflammatory drugs including COX inhibitors. The present results suggest that COX inhibitors are unlikely to suppress defence mechanisms associated with hBD-2 in airway epithelia. Recently it has been reported that inhibition of COX and lipoxygenase might be effective in treating sepsis-associated adult respiratory distress syndrome.[23] The present data might further support this treatment in terms of maintaining host defence.

In summary, dexamethasone inhibits hBD-2 gene expression induced by LPS. Both NF-κB and AP-1 transcription factors are essential for hBD-2 gene expression. Cyclooxygenase inhibitors fail to inhibit LPS-induced expression of hBD-2, suggesting that COX inhibitors are unlikely to suppress host defence associated with hBD-2. Glucocorticoid-induced down-regulation of hBD-2 may be related to GC-induced suppression of respiratory host defence. The inducible β-defensins including hBD-2 might provide a new therapeutic approach to GC-induced susceptibility to respiratory infection.